Abuja-Nigeria

DEPARTMENT OF PETROLEUM ENGINEERING

ENHANCED OIL RECOVERY IN HIGH VISCOUS RESERVOIR USING THE THERMAL PROCESS

A

THESIS

Presented to the Department of Petroleum Engineering

Of the African University of Science and Technology, Abuja

In Partial Fulfillment of the Requirements

For the Degree of

MASTER OF SCIENCE IN PETROLEUM ENGINEERING

By

APPIAH ELIZABETH AKONOBEA

[DECEMBER, 2014]

ENHANCED OIL RECOVERY IN HIGH VISCOUS RESERVOIR USING THE THERMAL PROCESS

A THESIS APPROVED BY THE PETROLEUM ENGINEERING DEPARTMENT

RECOMMENDED BY:

Thesis Supervisor:

Dr. Alpheus Igbokoyi

Committee Member:

Dr. Akin-Ojo Omololu

Committee Member:

Prof. David Ogbe

APPROVED BY:

Head Petroleum Engineering Department:

Professor Wumi Illedare

Chief Academic Officer:

Professor Charles Chidume

Date:

ABSTRACT

New sources of energy should be found to relieve the high demand of energy. Even though heavy oil and bitumen are difficult to produce due to their high viscosity which can be reduced by heating, with increased oil price, the production of these heavy oils are seen viable thus the need for a model that would help make predictions for the future and also take into consideration areal and vertical sweep of hydrocarbons (3D simulator). The ability to be able to optimize the interaction data and decision making during the life cycle of the field is critical. As a result of a heterogeneity of reservoirs, numerical simulators are used to obtain consistent and significant solutions.

For this work, a three-dimensional numerical reservoir simulator is developed for an expansion drive with a high viscous oil. A transient state heat system by conduction with an internal heat source is considered. A temperature simulator is first developed then coupled with a viscosity correlation after which it is then coupled with a diffusivity equation for a single phase flow of an expansion drive reservoir. All the governing equations are discretized using finite difference technique; iterative linear solver with the aid of MATLAB code is used to solve the system of linear equations.

This work aims to look at the effect of temperature on pressure drop through viscosity. It is realized that an increase in the heat source introduced a rise in temperature which in turn decrease the viscosity across the system. The pressure across the system is seen to be sustained even though it is declining thus the pressure being maintained.

ACKNOWLEDGEMENT

What shall I render unto the Lord for all He has done for me, I will lift His cup of victory and praise His name for He has done me well. Glory, Honor and adoration be unto Him.

My sincere appreciation goes to my main supervisor, Dr. Alpheus Igbokoyi for not only his world class supervision, patience, understanding and office but his thoughtful advices he gave me, I say 'Eshie'.

To my distinguished committee members; Dr. Akin-Ojo Omololu and Prof. David Ogbe whose computational modelling and reservoir simulation courses gave me the fundamentals of modelling and their quality supervision that they offered me, I say 'Ayekoo'. To my world class faculty for their undiluted knowledge they imparted, I wish to express my heartfelt gratitude.

To all my course mates for their support and time especially Mohammed Sani, Bismark Oteng, Olalekan Ladipo and Emmanuel Ofomena I say 'well done'. I wish also to say thank you to all the PhD students of AUST for their counsel and resources they gave me especially Edward Kofi Ampaw. To Dele Nurudeen, Yusif Shaidu and Lekan Keshiro for their time and energy, I am very grateful.

To all my wonderful church members for their prayers and support and also to friends far and near for their encouragement, I say 'Nnagodie'.

To my roommate, Monica Crankson, I would not have pulled through without your support, I say 'Medaase'.

Lastly to my family; Dad, Mum, Dan, Tina, Sammy, Christy, Edwin and the two Kofi's, for their undying love and support.

DEDICATION

This work is dedicated to my family; Mr. Kwadwo Appiah, Mrs. Wilhelmina Hesse-Appiah, Daniel Kwasi Appiah, Samuel Nyarko Appiah, Christy Adubea Appiah-Bonsu, Ernestina Effah-Appiah, Edwin Osei-Bonsu for their undying love, prayers and support and also to my two lovely nephews; Samuel Kofi Appiah and Wilhelm Kofi Appiah.

TABLE OF CONTENTS

LIST OF FIGURES

CHAPTER ONE

INTRODUCTION

1.1 General Introduction

Reservoirs act differently due to varying range of both rock and fluid properties and thus must be treated uniquely. During production, reservoirs are allowed to naturally produce their hydrocarbons until when production rates are mostly not economical viable then other support systems are used. Primary recovery is the natural stage of the reservoir to be able to produce without support thus depending on reservoir's internal energy. There are different drive mechanisms known as a results of different energy sources. The drive mechanism of a reservoir is not known in the earlier life of the production but can be seen from production data with time. The knowledge about the reservoir's drive mechanism can help improve reserves recovery and supervision during its middle and later life. The important drive mechanisms include: Rock and liquid expansion drive, solution gas/ depletion drive, Gas cap drive, Water drive, Combination drive and Gravity drainage drive.

Rock and liquid expansion drive has its oil existing at a higher pressure than the bubble point pressure and with only oil, connate water and the rocks. The rock and fluids expand as a result of their different compressibility as the reservoir pressure deplete. Formation compaction and expansion of different rock grains are some factors that affect reservoir rock compressibility. These factors are due to decrease of fluid pressure within the pore spaces which in turn reduce pore volume through porosity reduction. While the pore volume is reducing, the crude oil and water will be forced out of the pore space to the wellbore. Due to the compressibility (slightly) of both liquids and rocks, the reservoir will experience a rapid pressure decline. A constant gas-oil ratio

equal to gas solubility at bubble point pressure is typical of this drive mechanism. A small percentage of total oil in place is recovered due to the less efficiency of this drive.

Other recovery methods like Secondary and tertiary (Enhanced) recovery methods are employed to help improve the recovery of the remaining hydrocarbons by providing additional or sustaining the energy. The efficiency of an enhanced recovery method is a measure of its ability to provide greater hydrocarbon recovery than by natural depletion at economically attractive production rate (Marcel et al. 1980). It depends on reservoir characteristics and nature of displacing and displaced fluids. Enhanced recovery methods seeks to improve the sweep and displacement efficiency. It has been basically grouped into three types; namely chemical processes, miscible displacement processes and thermal processes. Thermal processes seeks to lower the viscosity of the fluid in place thus improving displacement and some of the processes are steam flooding and in-situ combustion. In order to manage and predict the performance of high viscous oil reservoir which is being heated using a heat probe, numerical reservoir simulation is needed thus the need for a three-dimensional numerical simulator for high viscous oil reservoir.

Reservoir simulation is the art of relating mathematics, physics, reservoir engineering, and computer encoding to predict hydrocarbon reservoir performance under different operating approaches (Aziz, K. and Settari, A. 1979).

Petroleum reservoir simulation is an approach whereby mathematical equations (model) or computable procedure are employed to infer the behavior of the real reservoir.

It is possible to obtain an exact solution for a few problems by direct integration of the differential equation (analytical solution). However, when analytical solutions breakdown, simple approximate methods (numerical solutions) are employed.

Today, numerical reservoir simulation is regularly used as a valuable tool to help make investment decisions on major exploitation and development projects. These decisions include determining commerciality, optimizing field development plans and initiating secondary and enhanced oil recovery methods on major oil and gas projects. Proper planning is made possible by use of reservoir simulation; it can be used effectively in the early stages of development before the pool is placed on production so that unnecessary expenditures can be avoided.

1.2 Problem definition

Heavy oil reservoirs cannot be easily produced due to their high viscosities which in turn inhibit mobility of hydrocarbons therefore enhanced oil recovery like thermal recovery method is employed to help decrease the viscosity drag effect of the hydrocarbons. These recovery methods are capital intensive and as such need intensive studies and forecast about their outcomes therefore the need for a numerical reservoir simulator which can be one-dimensional (1-D), two-dimensional (2-D) and three-dimensional (3-D). With the 3-D model, it gives full description of the real situation by accounting for both areal and vertical sweep efficiencies which neither 1-D nor 2-D models can give thus the need for a 3-D numerical simulator for high viscous oil reservoir.

1.3 Objectives

Below are the outlined objectives for the work:

- To derive and solve a heat equation for conduction with a heat source using finite difference method.

- Using a viscosity correlation, predict the viscosity dependence on temperature for a high viscous volumetric oil reservoir.
- To derive and solve diffusivity equation for single phase flow using finite difference method.
- To develop a 3-D numerical simulator for high viscous oil reservoir combining the heat, viscosity and diffusivity equations using MATLAB.
- To use the developed simulator to predict temperature distribution and pressure decline.

1.4 Scope and limitation of this work

This work is limited to (the development of a numerical simulator for) heavy oil reservoir with expansion drive as it primary drive for recovery.

1.5 Organization of thesis

The thesis is structured in this manner:

- Chapter two gives a brief evaluation of drive mechanisms, enhanced oil recovery and thermal recovery. Numerical reservoir simulation and numerical methods for discretization of the equations governing heat transfer and flow in subsurface reservoirs, including benefits and limitations of finite difference method are reviewed. Also in review is simple iterative method and use of MATLAB programming in reservoir simulation.
- Chapter three presents the methodology employed in this study; mathematical, numerical and computer models formulations.
- In Chapter four contains the discussion of the results.

- Chapter five draws logical conclusions based on the simulator results, and makes useful recommendations for further studies.

CHAPTER TWO

LITERATURE REVIEW

2.1 Natural Drive Mechanism

Each reservoir is composed of a unique combination of geometric form, geological rock properties, fluid characteristics, and drive mechanism (primary). The recovery of oil by any of the natural drive mechanisms is called primary recovery thus no energy supplement. Although no two reservoirs are identical in all aspects, they can be grouped according to the primary recovery mechanism by which they produce (Ahmed 2006). There are basically six driving mechanisms that provide the natural energy necessary for oil recovery:

- Depletion drive (This type of drive has its main source of energy being due to gas liberation from the crude oil and expansion of the solution gas as the reservoir pressure is reduced.)
- Gas cap drive (This drive is identified by the presence of a gas cap with little or no water drive. The reservoir pressure decline is slow due to the ability of the gas to expand.)
- Water drive (Most reservoirs are bounded on a portion or all the edges by water bearing rocks called aquifers. These aquifers help provide energy to push the hydrocarbons. There are bottom water and edge water occurring in this drive.)
- Gravity drainage drive (This drive is as result of differences in densities of the reservoir fluids)
- Combination drive (This drive can chain two or more of the above drives)

2.1.1 Rock and Liquid Expansion Drive

Expansion occurs as the reservoir undergoes a pressure depletion. In such conditions when no external influx is present, the reservoir fluid essentially displaces itself. For under saturated oil reservoirs, the liquid phase expansion contributes only a little to oil recovery, since oil compressibility is usually very low, especially in medium to heavy gravity oils.

In under saturated oil reservoirs producing by rock and fluid expansion, the pressure declines very rapidly due to the rock and liquid being slightly compressible while the producing Gas-Oil-Ratio (GOR) remains constant. Fluid and rock expansion is naturally the least efficient drive mechanism for oil reservoirs especially heavy oil reservoirs and thus the need to supplement with external energy sources.

2.2 Enhanced Oil Recovery Methods

The process of producing hydrocarbons by methods other than the normal methods is called enhanced oil recovery (EOR). It also includes re-pressurizing schemes with gas and water. An EOR method should generate an incremental oil recovery. Incremental oil is designated as oil produced higher than the projected production from the reservoir without the EOR method (Ezekwe 2011). Heavy oil and oil sands that cannot be produced by conventional methods. Applications of EOR methods such as thermal process, can improve oil recovery from these types of reservoirs. Figure 2.2 shows a modified diagram of EOR methods (Arfo 2014). They can be classified into the following processes;

2.2.1 Miscible Gas Injection Processes

A fluid/solvent that dissolves the reservoir oil is introduced into the reservoir such as Alcohol, Refined hydrocarbons, LPG or exhaust gas. This process improve recovery efficiency by reducing viscosity, condensing and vaporizing gas drive and displacing oil from pore spaces. This process can further be grouped into CO_2 flooding, miscible hydrocarbon displacement and inert gas flooding.

2.2.2 Chemical Processes

Chemicals are injected into the reservoir to alter fluid or rock properties. Candidate reservoir should have adequate injectivity since the injected fluids have lower mobility. Active water drive reservoirs should be avoided as they have potential for low residual oil saturation. Reservoirs with gas caps may not be good candidates for this method because mobilized oil might re- saturate the gas cap. Reservoir formations rich in clay should be avoided because they increase adsorption of the injected chemical. Moderate salinity brine reservoirs are preferable because high salinity concentration interact unfavorably with the injected chemicals. Under these process, there are five different processes namely; Polymer flooding, Surfactant flooding, Alkaline flooding, Surfactant/ Polymer flooding and Alkaline/ Surfactant/ Polymer Flooding (Arfo 2014).

2.2.3 Thermal processes

Thermal EOR processes are defined to include all processes that supply heat energy to the rocks and fluids contained in a reservoir thereby enhancing the ability of oil (including other fluids) to flow by primarily reducing its viscosity. The heat cause thermal expansion which affects the

relative permeability and also sometimes cause the activation of solution gas drive. The oil caused to flow by the supply of thermal energy is produced through nearby wells. There are three categories of thermal methods:

2.2.3.1 Cyclic Steam Injection (Steam Stimulation, Steam Soak or Huff and Puff): In this process, steam is injected down a producing well to heat up the area around the well bore and increase recovery of the oil immediately adjacent to the well. After injection of short period, the well is placed back on production. This is essentially a well bore stimulation technique, each well responding independently. This process is repeated until production falls below a profitable level.

2.2.3.2 Steam Drive (Steam Flooding, Continuous Steam Injection): Steam is injected through injection wells and the oil is displaced to surrounding producing wells as in conventional fluid injection operations. Less viscous crude oils can be steam flooded if they don't respond to water. This method reduces viscosity, bring about steam distillation and supplies pressure to drive oil to the producing well.

2.2.3.3 In-Situ Combustion (Fire-flood): This process involves in-situ combustion of portions of the oil. There are two mechanisms involved namely forward and backward combustion. Air is pumped into the reservoir which either self-ignites or is ignited, depending on reservoir temperature and composition. This heat produced is used to thin the oil and permit it to flow more easily towards the producing wells (Arfo 2014).

Most of these processes are modelled due to its capital involvement thus the need for reservoir simulation to help predict the outcome of such processes.

2.2.3.4 Heavy Oil recovery methods

These methods include:

- Steam Assisted Gravity Drive (SAGD): It's an advanced form of steam Stimulation involving a pair of horizontal wells, one 4 to 6 metres above the other. The upper one is used for injecting high pressure steam, which heats the oil and reduces its viscosity. The heated oil drains into the lower wellbore and is produced from there.
- Toe-to-Heel Air Injection (THAI), is a proposed method of recovery that combines a vertical air injection well with a horizontal production well (Arfo, 2014).

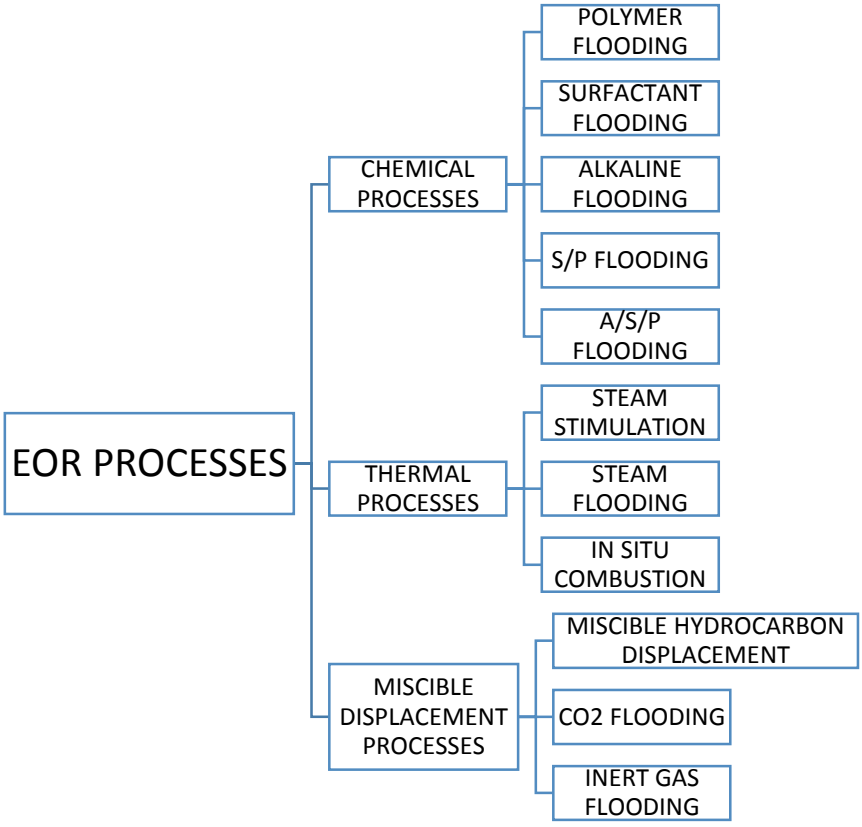

Figure 2.2: A Diagram showing EOR Methods.

2.3 Numerical Reservoir Simulation

Simulation is the only way to describe quantitatively the flow of multi phases in heterogeneous reservoir having a production schedule determined not only by the properties of the reservoir, but also by market demand, investment strategy and government regulations (Mattax & Dalton 1990). There are other methods of forecasting reservoir performance which include experimental, analogical and mathematical methods. Over the past few years, the interest in the numerical modeling of fluid displacement processes in porous media has been rising rapidly. The emergence of complex enhanced recovery procedures in the field of hydrocarbon extraction techniques has emphasized the need for sophisticated mathematical tools, capable of modeling intricate chemical and physical phenomena and sharply changing fluid interfaces. Figure 2.3 shows a schematic diagram of a numerical reservoir simulation process (Cheng Y. 2002).

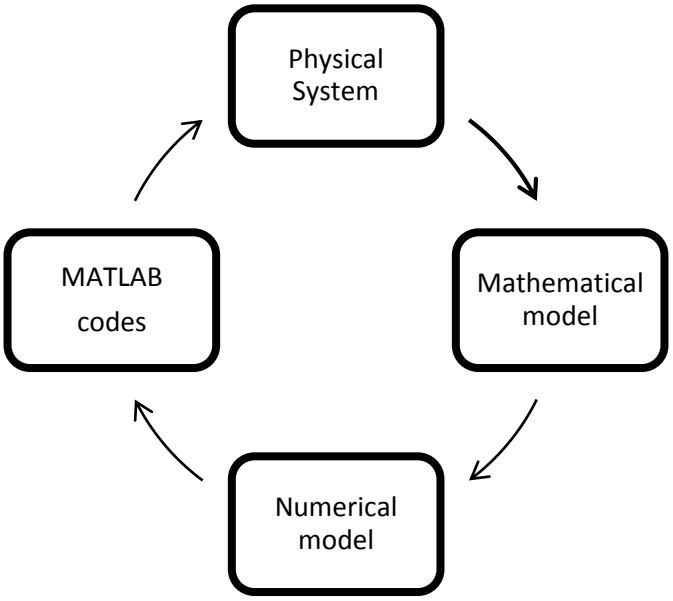

Figure 2.3.1: Schematic diagram of the numerical reservoir simulation process

Reservoir simulation is needed for there to be accurate performance predictions for a hydrocarbon reservoir under different operating conditions. Since hydrocarbon recovery project involves a lot

of capital investment, the risk associated with the project must be fully assessed and minimized. All these assessment and predictions are based on the software being used and the input data. The success of reservoir modelling is based on the ability of the equations being used to represent both the physics of the fluid flow and equilibrium in the reservoir and well system; and the ability of the grid properties to represent the dimensional descriptions (Archer 1983).

Ogbe, David (2014) gives reservoir simulators classification based on:

- Type of reservoir or its fluids to be simulated (Gas, Black oil, naturally fractured).
- Recovery process to be used (chemical, miscible, thermal, polymer).
- Geometry or dimensions (Cartesian, radial, 1D, 2D, 3D).
- Special purpose / function (asphaltene deposition, phase behavior).
- Phases (single phase, 2 phase, 3 phase)

From the classification based on dimensions, there are:

- Figure 2.3.2a shows a one dimensional model that can be used to simulate single well operation, sections of the reservoir and reef structures among others.
- Figure 2.3.2 b & c shows a two dimensional model that can be used to describe the areal performance or to stimulate the vertical conformance in a reservoir. This can be used in cross sectional analysis of a reservoir and also to check heterogeneity effect on frontal displacement.
- Figure 2.3.2d shows a three dimensional model that can account for both areal and vertical conformance all together. It can handle all types of simulation studies.

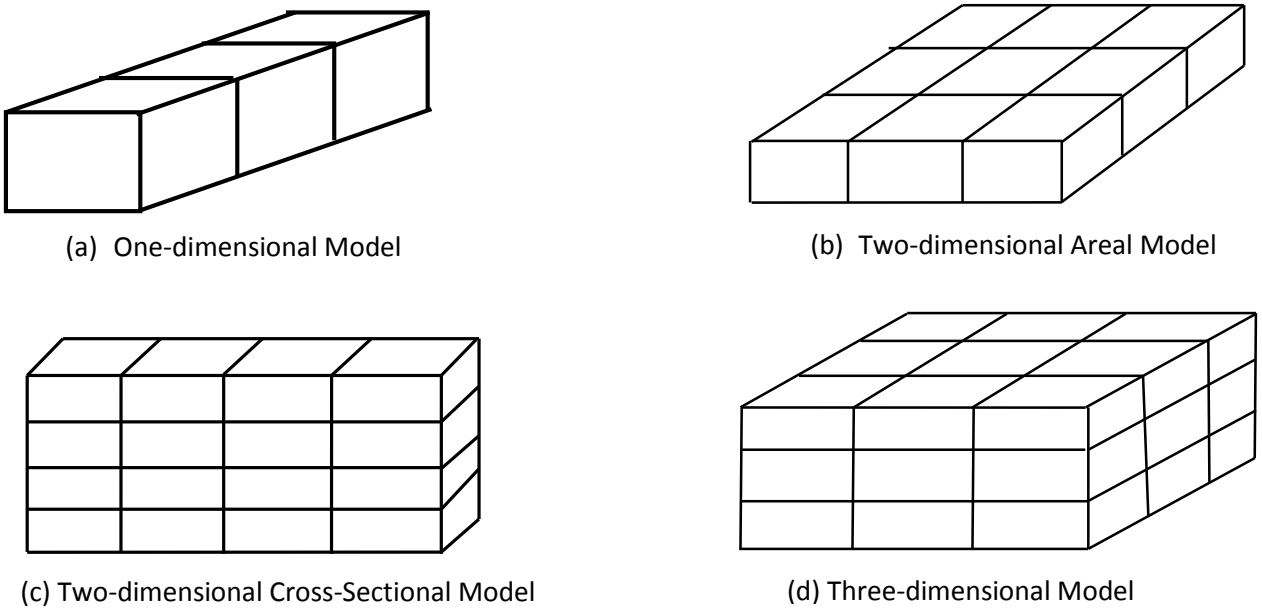

Figure 2.3.2: A schematic Diagram of reservoir models based on dimension.

The need for the selection of a suitable tool is important in order not to choose any tool that would make available misrepresentative results if not used successfully. A three dimensional model is known to be the best tool to both assess the past performance and forecast the future performance of a reservoir due to its combination of areal, vertical conformance and gravity effects , all in one model. Under numerous operating conditions, a precise numerical model of a reservoir can be developed to forecast aftermaths and performance in order to make quality decisions regarding hydrocarbons recovery (Dele et al. 2014). This work seeks to develop a three-dimensional numerical simulator for high viscous expansion drive reservoirs.

2.4 Numerical Methods

Numerical methods use high-speed computers to solve the mathematical equations describing the physical behavior of the processes in a reservoir to obtain a numerical solution to the reservoir behavior of the field. It is possible to obtain an exact solution for a few problems by direct

integration of the differential equation (analytical solution). However, when analytical solutions breakdown, simple approximate methods (numerical solutions) are employed. There are three methods available for discretization (process of converting partial differential equation, PDE into algebraic equations); the Taylor series method, the integral method and the variational method (Abou-Kassem et al, 2006).

The solution of linear and non – linear boundary value problems (BVPs) for numerical are shown below (Omololu, 2014):

i. Perturbation

ii. Power series

iii. Probability schemes

iv. Method of weighted residuals (MWR)

v. Ritz method

vi. Finite difference method/technique (FDM)

vii. Finite element method (FEM)

2.4.1 Finite Difference Method (FDM)

Finite difference approach is the most commonly used numerical method in reservoir simulation. It is a numerical technique used to approximate continuous (ordinary and partial) differential equations to discretize form. Simplicity and ease of extension from 1D to 2D and 3D are advantages listed by Abbas Firoozabadi et al (2000). Grid dependency and numerical dispersion are some of the main disadvantages of this method. Heat problems are solved using this method. Some applications in the oil industry are solving oil recovery processes and fluid flow problems in porous media.

In using this method, a grid system is made out of the reservoir to be modeled, which is used to make spatial discretization. The approximations made require smaller time step of the total simulation time. Point-distributed and block-centered grid are the two basic finite difference grids.

2.5 Linear Solvers in Reservoir Simulators

The linear solver is an essential component in a reservoir simulator. It is used to solve the discretized nonlinear partial differential equations. These equations describe mass balances on the individual components treated in the model. For non-isothermal problems, an energy balance is added to the system. There are two methods of solving the equations resulting from the finite difference approximation for a system:

2.5.1 Direct Solution Methods

This method theoretically give an exact solution in a finite number of steps. Due to rounding errors, this is not mostly true thus an error made in one step spread in the remaining steps. Solving an equation system by means of matrix decompositions can be classified as a direct method (Cramer's rule, Gaussian Elimination, Matrix inversion, Matrix factorization). Direct solver has a limitation of computer storage capacity due to the storage of both coefficient matrix and right vector throughout the solution formulation. Figure 2.5.1 shows a modified diagram representing a direct solution method (Ogbe 2014)

Figure 2.5.1: Schematic diagram of steps involving direct solution method.

2.5.2 Iterative Solution Methods

Iterative methods construct a series of solution approximations that under some assumptions converges to the solution of the system. They are self-correcting but rather slower since they would undergo a large number of iterations required. Examples of iterative methods include: Jacobi iteration, Gauss-Siedel, Successive Over-Relaxation (SOR), Strongly Implicit Procedure (SIP), Matrix Conditioning and Conjugate Gradient Method. Iterative solution methods do not always converge to the solution. Figure 2.5.2 shows a schematic representation of the iterative solution method (Ogbe, 2014).

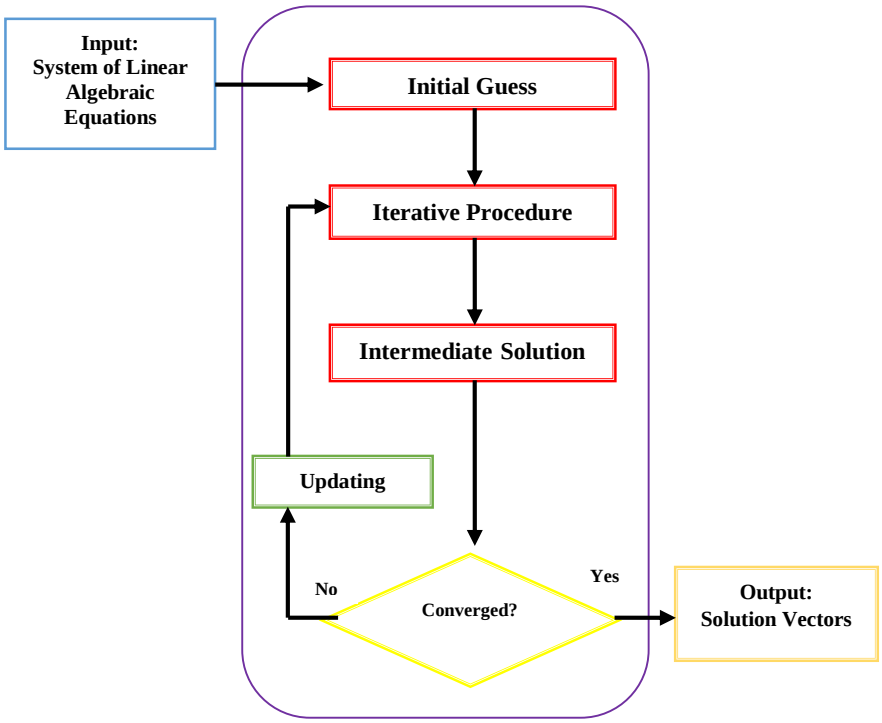

Figure 2.5.2: A Schematic Representation of the iterative solution method.

2.5.2.1 Simple Iterative method

This is a fairly simple method, which requires the problem to be written in the form

$x = f(x)$ for some function $f(x)$. We start with an initial guess to the solution, x_1 and then calculate a new estimate as $x_2 = f(x_1)$. This process is continued, at each step generating a new approximation $x_{n+1} = f(x_n)$. The iterations are stopped when the difference between successive estimates becomes less than some prescribed convergence criterion ε. i.e. when $|x_{n+1} - x_n| < \varepsilon$

If the process is convergent, then taking a smaller value for ε results in a more accurate solution, although more iterations will need to be performed.

2.6 MATLAB Programming

MATLAB® is a high-level language and interactive environment for numerical computation, visualization, and programming. Using MATLAB, you can analyze data, develop algorithms, and create models and applications. The language, tools, and built-in math functions enable you to explore multiple approaches and reach a solution faster than with spreadsheets or traditional programming languages, such as C/C++ or Java™. In academia, MATLAB has gradually taken over most of the scientific programming work with its interactive easy to use features. Matlab is used in solving a wide range of mathematical and engineering problems. According to Matlab official product website, some key features of Matlab are listed below:

- High-level language for numerical computation, visualization, and application development
- Interactive environment for iterative exploration, design, and problem solving
- Mathematical functions for linear algebra, statistics, Fourier analysis, filtering, optimization, numerical integration, and solving ordinary differential equations
- Built-in graphics for visualizing data and tools for creating custom plots

- Development tools for improving code quality and maintainability and maximizing performance
- Tools for building applications with custom graphical interfaces
- Functions for integrating MATLAB based algorithms with external applications and languages such as C, Java, .NET, and Microsoft® Excel®

MATLAB is being gradually accepted in and used in various industries as well. It is being widely recognized for its easy interface and time saving features, and also Reservoir Modeling is now being carried out using MATLAB.

CHAPTER THREE

METHOD USED

3.1 Development of the Simulator

The following itemized stages were used in developing the three dimensional numerical oil reservoir simulator:

- Derive a heat partial differential equations of the model by conduction based on the rock and fluid properties of the reservoir.
- Discretize the derived heat diffusion equations in both space and time to obtain a system of linear equations.
- Establish the stability of the equations using the Crank Nicolson scheme.
- Write Codes for the discretized equations using MATLAB Programming.
- Couple the temperatures from the heat model with a viscosity model using MATLAB Programming.
- Derive a diffusivity partial differential equations for an expansion drive reservoir.
- Discretize the derived diffusivity equation in both space and time to obtain another system of equations.
- Establish these equations' stability using Crank Nicolson scheme.
- Write Codes for the systems of equations using MATLAB Programming.
- Validate the simulator using Base case results.

In the development of this reservoir simulator, three main models were used; Mathematical model, Numerical model and Computer model (MATLAB code)

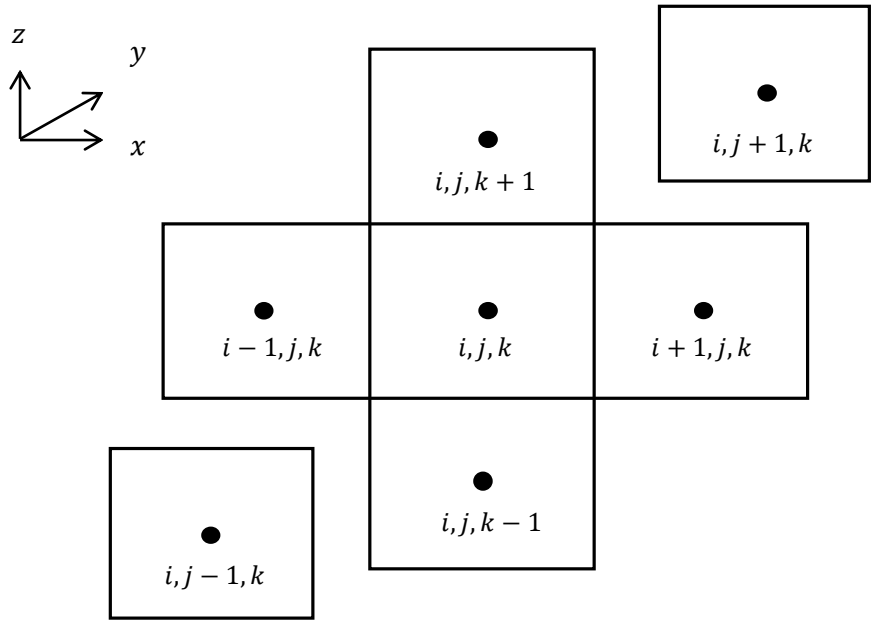

Figure 3.1: A numerical stencil for a three-dimensional oil reservoir block

3.2 Heat Model

Whenever there exist a temperature difference in a medium or between media, heat transfer occurs (Incropera et al., 1990). When a temperature gradient exists in a stationary medium, which may be a solid or a fluid, the heat transfer is termed as conduction. Figure 3.2 represents how heat is transfer from one end to another through a medium till equilibrium.

Figure 3.2.1: A diagrammatic representation of conduction.

3.2.1 Mathematical Model

The model is developed using heat by conduction with a heat source and inculcating the appropriate initial and boundary conditions that represents the performance of the reservoir. The model is basically governed by Fourier's law.

Basic Assumptions

- No-flow reservoir boundary condition
- Internal Heat Generation
- Transient State conditions
- Homogenous Reservoir with constant properties
- Uniform grid size
- Constant average thermal conductivity , specific heat capacity and density

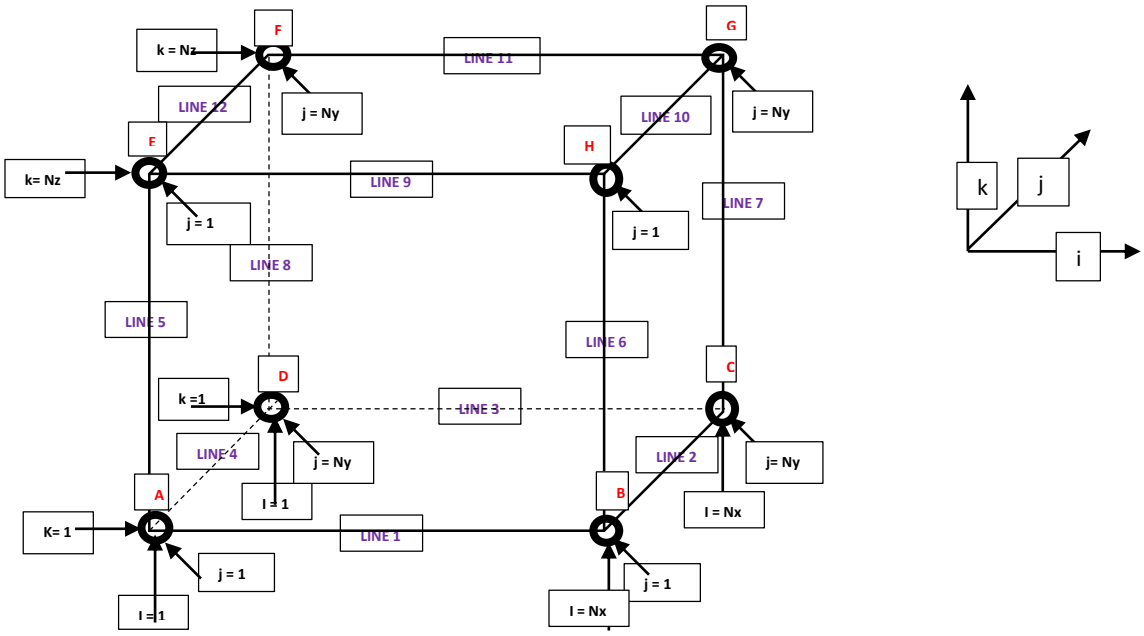

Figure 3.2.2: A diagrammatic representation of the volumetric system.

3.2.1.1 Derivation of the heat equation.

$$\Delta Q = \Delta m C_p \Delta T \qquad (3.0)$$

Where $m = \rho V$

$\Delta m = \rho dV$ for a small portion in the bigger portion. (3.1a)

$$\Delta Q = (\rho dV) C_p (T - T_o)$$

$$Q = \int_v (\rho dV)\, C_p (T - T_o) \quad (3.2)$$

$$\frac{dQ}{dt} = G - R \quad (3.2a)$$

$$R = \int_s q.\, dS = \int_v \nabla q.\, dV \quad (3.2b)$$

$$G = \int_v g.\, dV \quad (3.2c)$$

Where S = surface area

V = volume of the system,

T is temperature

x, y and z are the Cartesian directions,

k is thermal conductivity of the system,

α is thermal diffusivity of the system,

C_p is specific heat at constant pressure,

ρ is density of material used,

Q is amount of heat in the system,

R is heat flowing out of the system,

G is heat generated within the system.

$$\frac{d}{dt}\left[\int_v \rho C_p (T - T_o) dV\right] = \int_v g.\, dV - \int_v \nabla q.\, dV \quad (3.3)$$

$$\int_v dV \rho C_p \frac{\partial T}{\partial t} = \int_v dV (g - \nabla q)$$

$$\int_v dV \left[\rho C_p \frac{\partial T}{\partial t} - g + \nabla q\right] = 0$$

Since dV is an arbitrary volume, integrand = 0.

$$\rho C_p \frac{\partial T}{\partial t} - g + \nabla q = 0 \quad (3.4)$$

$$q = -k\nabla T \tag{3.4a}$$

$$\rho C_p \frac{\partial T}{\partial t} = g + k\nabla^2 T \tag{3.5}$$

$$\nabla^2 T = \frac{\partial^2 T}{\partial x^2} + \frac{\partial^2 T}{\partial y^2} + \frac{\partial^2 T}{\partial z^2} \tag{3.5a}$$

$$\frac{\partial T}{\partial t} = \frac{g}{\rho C_p} + \frac{k}{\rho C_p}\nabla^2 T \tag{3.6}$$

$$\alpha = \frac{k}{\rho C_p} \tag{3.6a}$$

$$\frac{\partial T}{\partial t} = \alpha\nabla^2 T + \frac{g}{\rho C_p} \tag{3.7}$$

3.2.2 Numerical Model

The equation constituting the mathematical model of the reservoir is complex to be solved by analytical method. The finite difference method is used to put the equation in a form that can be solved digitally by a computer. This process involves spatial and time derivative discretization.

3.2.2.1 Spatial Discretization

The general PDE for a single phase written in Cartesian coordinates as:

$$\frac{\partial T}{\partial t} = \alpha\left[\frac{\partial^2 T}{\partial x^2} + \frac{\partial^2 T}{\partial y^2} + \frac{\partial^2 T}{\partial z^2}\right] + \frac{g}{\rho C_p} \tag{3.8}$$

In discretizing the right hand side using central difference method (which is mostly accurate)

$$\frac{\partial^2 T}{\partial x^2}_{i,j,k} = \frac{\partial}{\partial x}\left[\frac{\partial T}{\partial x}\right] \tag{3.8a}$$

$$\text{If } \frac{\partial T}{\partial x} = \frac{T_{i+1/2,j,k} - T_{i-1/2,j,k}}{\Delta x} \tag{3.8b}$$

$$\text{Thus } \frac{\partial^2 T}{\partial x^2} = \frac{\partial}{\partial x}\left[\frac{T_{i+1/2,j,k} - T_{i-1/2,j,k}}{\Delta x}\right]$$

$$\frac{\partial^2 T}{\partial x^2}_{i,j,k} = \frac{\left[\frac{T_{i+1,j,k} - T_{i,j,k}}{\Delta x}\right] - \left[\frac{T_{i,j,k} - T_{i-1,j,k}}{\Delta x}\right]}{\Delta x}$$

$$\frac{\partial^2 T}{\partial x^2}_{i,j,k} = \frac{T_{i+1,j,k} - 2T_{i,j,k} + T_{i-1,j,k}}{(\Delta x)^2} \tag{3.8c}$$

Therefore

$$\frac{\partial^2 T}{\partial y^2}_{i,j,k} = \frac{T_{i,j+1,k}-2T_{i,j,k}+T_{i,j-1,k}}{(\Delta y)^2} \quad (3.8d)$$

$$\frac{\partial^2 T}{\partial z^2}_{i,j,k} = \frac{T_{i,j,k+1}-2T_{i,j,k}+T_{i,j,k-1}}{(\Delta z)^2} \quad (3.8e)$$

$$\frac{\partial T}{\partial t} = \alpha\left[\left(\frac{T_{i+1,j,k}-2T_{i,j,k}+T_{i-1,j,k}}{(\Delta x)^2}\right)+\left(\frac{T_{i,j+1,k}-2T_{i,j,k}+T_{i,j-1,k}}{(\Delta y)^2}\right)+\left(\frac{T_{i,j,k+1}-2T_{i,j,k}+T_{i,j,k-1}}{(\Delta z)^2}\right)\right]+\frac{g}{\rho C_p} \quad (3.9)$$

3.2.2.2 Time Discretization

For the left hand side of the equation, using backward difference approximation with a base time level at n+1;

$$\frac{\partial T}{\partial t} = \frac{T_{i,j,k}^{n+1}-T_{i,j,k}^{n}}{\Delta t} \quad (3.10)$$

Combining the left hand side and right hand side with crank Nicolson algorithm which is an implicit scheme formulation.

$$\frac{T_{i,j,k}^{n+1}-T_{i,j,k}^{n}}{\Delta t} = \alpha\left\{\left(\left(\frac{T_{i+1,j,k}^{n+1}-2T_{i,j,k}^{n+1}+T_{i-1,j,k}^{n+1}}{(\Delta x)^2}\right)+\left(\frac{T_{i,j+1,k}^{n+1}-2T_{i,j,k}^{n+1}+T_{i,j-1,k}^{n+1}}{(\Delta y)^2}\right)+\left(\frac{T_{i,j,k+1}^{n+1}-2T_{i,j,k}^{n+1}+T_{i,j,k-1}^{n+1}}{(\Delta z)^2}\right)\right)+\right.$$

$$\left.\left(\left(\frac{T_{i+1,j,k}^{n}-2T_{i,j,k}^{n}+T_{i-1,j,k}^{n}}{(\Delta x)^2}\right)+\left(\frac{T_{i,j+1,k}^{n}-2T_{i,j,k}^{n}+T_{i,j-1,k}^{n}}{(\Delta y)^2}\right)+\left(\frac{T_{i,j,k+1}^{n}-2T_{i,j,k}^{n}+T_{i,j,k-1}^{n}}{(\Delta z)^2}\right)\right)\right\}+\frac{g}{\rho C_p} \quad (3.11)$$

Where i, j, k are the coordinate representations in the x, y and z directions respectively.

$$\frac{T_{i,j,k}^{n+1}-T_{i,j,k}^{n}}{\Delta t} = \alpha\left(\left(\frac{T_{i+1,j,k}^{n+1}-2T_{i,j,k}^{n+1}+T_{i-1,j,k}^{n+1}+T_{i+1,j,k}^{n}-2T_{i,j,k}^{n}+T_{i-1,j,k}^{n}}{(\Delta x)^2}\right)+\left(\frac{T_{i,j+1,k}^{n+1}-2T_{i,j,k}^{n+1}+T_{i,j-1,k}^{n+1}T_{i,j+1,k}^{n}-2T_{i,j,k}^{n}+T_{i,j-1,k}^{n}{}^{+}}{(\Delta y)^2}\right)+\right.$$

$$\left.\left(\frac{T_{i,j,k+1}^{n+1}-2T_{i,j,k}^{n+1}+T_{i,j,k-1}^{n+1}+T_{i,j,k+1}^{n}-2T_{i,j,k}^{n}+T_{i,j,k-1}^{n}}{(\Delta z)^2}\right)\right)+\frac{g}{\rho C_p} \quad (3.12)$$

Let $[(\Delta x)^2.(\Delta y)^2.(\Delta z)^2] = D$ (3.12a)

$[(\Delta y)^2.(\Delta z)^2] = Dx$ (3.12b)

$[(\Delta x)^2.(\Delta z)^2] = Dy$ (3.12c)

$[(\Delta x)^2.(\Delta y)^2] = Dz$ (3.12d)

Multiply Eqn 3.12 through by Eqn 3.12a

$$D\left(\frac{T_{i,j,k}^{n+1}-T_{i,j,k}^{n}}{\Delta t}\right)=\alpha\left(Dx\left(T_{i+1,j,k}^{n+1}-2T_{i,j,k}^{n+1}+T_{i-1,j,k}^{n+1}+T_{i+1,j,k}^{n}-2T_{i,j,k}^{n}+T_{i-1,j,k}^{n}\right)+Dy\left(T_{i,j+1,k}^{n+1}-\right.\right.$$

$$\left.2T_{i,j,k}^{n+1}+T_{i,j-1,k}^{n+1}+T_{i,j+1,k}^{n}-2T_{i,j,k}^{n}+T_{i,j-1,k}^{n}\right)+Dz\left(T_{i,j,k+1}^{n+1}-2T_{i,j,k}^{n+1}+T_{i,j,k-1}^{n+1}+T_{i,j,k+1}^{n}-2T_{i,j,k}^{n}+\right.$$

$$\left.\left.T_{i,j,k-1}^{n}\right)\right)+\frac{g}{\rho C_p}D \qquad (3.13)$$

Simplifying the equation:

$$\frac{D}{\alpha\Delta t}\left(T_{i,j,k}^{n+1}-T_{i,j,k}^{n}\right)=\left(Dx\left(T_{i+1,j,k}^{n+1}-2T_{i,j,k}^{n+1}+T_{i-1,j,k}^{n+1}+T_{i+1,j,k}^{n}-2T_{i,j,k}^{n}+T_{i-1,j,k}^{n}\right)+Dy\left(T_{i,j+1,k}^{n+1}-\right.\right.$$

$$\left.2T_{i,j,k}^{n+1}+T_{i,j-1,k}^{n+1}+T_{i,j+1,k}^{n}-2T_{i,j,k}^{n}+T_{i,j-1,k}^{n}\right)+Dz\left(T_{i,j,k+1}^{n+1}-2T_{i,j,k}^{n+1}+T_{i,j,k-1}^{n+1}+T_{i,j,k+1}^{n}-2T_{i,j,k}^{n}+\right.$$

$$\left.\left.T_{i,j,k-1}^{n}\right)\right)+\frac{g}{k}D \qquad (3.14)$$

3.2.3 Computer Model

In coding the equation,

Let $\beta=\frac{D}{\alpha\Delta t}$ (3.14a)

$S=\frac{gD}{k}$ (3.14b)

Using $M=(k-1)N_xN_y+(j-1)N_x+i,$ (3.14c)

$i, j, k = m$ (3.14d)

$i\pm1, j, k=m\pm1$ (3.14e)

$i, j\pm1, k=m\pm N_x$ (3.14f)

$i, j, k\pm1=m\pm N_2$ (3.14g)

Where N_2 is N_xN_y (3.14h)

Applying no flow boundary conditions:

$$\frac{\partial T}{\partial x}=0 \qquad (3.15)$$

$$\frac{T_{x+\Delta x}-T_{x-\Delta x}}{2\Delta x}=0\rightarrow T_{x+\Delta x}=T_{x-\Delta x}$$

$$\frac{\partial T}{\partial x} \rightarrow T_{m+1} = T_{m-1} \quad (3.15a)$$

$$\frac{\partial T}{\partial y} \rightarrow T_{m+N_x} = T_{m-N_x} \quad (3.15b)$$

$$\frac{\partial T}{\partial z} \rightarrow T_{m+N_2} = T_{m-N_2} \quad (3.15c)$$

3.2.3.1 For interior nodes

$$\beta(T_m^{n+1} - T_m^n) = \{\left[Dx(T_{m+1}^{n+1} - 2T_m^{n+1} + T_{m-1}^{n+1}) + Dy\left(T_{m+N_x}^{n+1} - 2T_m^{n+1} + T_{m-N_x}^{n+1}\right) + Dz\left(T_{m+N_2}^{n+1} - 2T_m^{n+1} + T_{m-N_2}^{n+1}\right)\right] + \left[Dx(T_{m+1}^{n} - 2T_m^{n} + T_{m-1}^{n}) + Dy\left(T_{m+N_x}^{n} - 2T_m^{n} + T_{m-N_x}^{n}\right) + Dz\left(T_{m+N_2}^{n} - 2T_m^{n} + T_{m-N_2}^{n}\right)\right]\} + S(m)$$

$$(\beta + 2Dx + 2Dy + 2Dz)T_m^{n+1} = \{\left[Dx(T_{m+1}^{n+1} + T_{m-1}^{n+1} + T_{m+1}^{n} + T_{m-1}^{n}) + Dy\left(T_{m+N_x}^{n+1} + T_{m-N_x}^{n+1} + T_{m+N_x}^{n} + T_{m-N_x}^{n}\right) + Dz\left(T_{m+N_2}^{n+1} + T_{m-N_2}^{n+1} + T_{m+N_2}^{n} + T_{m-N_2}^{n}\right)\right] + [\beta - 2Dx - 2Dy - 2Dz]T_m^{n}\} + S(m) \quad (3.17)$$

Rearranging Eqn 3.17;

$$T_m^{n+1} = \left\{\left[\left[Dx(T_{m+1}^{n+1} + T_{m-1}^{n+1} + T_{m+1}^{n} + T_{m-1}^{n}) + Dy\left(T_{m+N_x}^{n+1} + T_{m-N_x}^{n+1} + T_{m+N_x}^{n} + T_{m-N_x}^{n}\right) + Dz\left(T_{m+N_2}^{n+1} + T_{m-N_2}^{n+1} + T_{m+N_2}^{n} + T_{m-N_2}^{n}\right)\right] + [\beta - 2Dx - 2Dy - 2Dz]T_m^{n}\right] + S(m)\right\}/(\beta + 2Dx + 2Dy + 2Dz) \quad (3.18)$$

Special Points

There are 26 special points which are treated differently due to the no flow boundary condition and these include 6 faces, 8 corners and 12 lines.

3.2.3.2 For the corners,

A i=1, j=1, k=1

$$T_m^{n+1} = \frac{\left\{\left[\left[2Dx\left(T_{m+1}^{n+1}+T_{m+1}^{n}\right)+2Dy\left(T_{m+N_x}^{n+1}+T_{m+N_x}^{n}\right)+2Dz\left(T_{m+N_2}^{n+1}+T_{m+N_2}^{n}\right)\right]+[\beta-2Dx-2Dy-2Dz]T_m^{n}\right]+S(m)\right\}}{(\beta+2Dx+2Dy+2Dz)} \quad (3.19)$$

E i=1, j=1, k= N_z

$$T_m^{n+1} = \frac{\left\{\left[\left[2Dx\left(T_{m+1}^{n+1}+T_{m+1}^{n}\right)+2Dy\left(T_{m+N_x}^{n+1}+T_{m+N_x}^{n}\right)+2Dz\left(T_{m-N_2}^{n+1}+T_{m-N_2}^{n}\right)\right]+[\beta-2Dx-2Dy-2Dz]T_m^{n}\right]+S(m)\right\}}{(\beta+2Dx+2Dy+2Dz)} \quad (3.20)$$

D i=1, j=N_y, k=1

$$T_m^{n+1} = \frac{\left\{\left[\left[2Dx\left(T_{m+1}^{n+1}+T_{m+1}^{n}\right)+2Dy\left(T_{m-N_x}^{n+1}+T_{m-N_x}^{n}\right)+2Dz\left(T_{m+N_2}^{n+1}+T_{m+N_2}^{n}\right)\right]+[\beta-2Dx-2Dy-2Dz]T_m^n\right]+S(m)\right\}}{(\beta+2Dx+2Dy+2Dz)} \quad (3.21)$$

F i=1, j=N_y, k=N_z

$$T_m^{n+1} = \frac{\left\{\left[\left[2Dx\left(T_{m+1}^{n+1}+T_{m+1}^{n}\right)+2Dy\left(T_{m-N_x}^{n+1}+T_{m-N_x}^{n}\right)+2Dz\left(T_{m-N_2}^{n+1}+T_{m-N_2}^{n}\right)\right]+[\beta-2Dx-2Dy-2Dz]T_m^n\right]+S(m)\right\}}{(\beta+2Dx+2Dy+2Dz)} \quad (3.22)$$

B i=N_x, j=1, k=1

$$T_m^{n+1} = \frac{\left\{\left[\left[2Dx\left(T_{m-1}^{n+1}+T_{m-1}^{n}\right)+2Dy\left(T_{m+N_x}^{n+1}+T_{m+N_x}^{n}\right)+2Dz\left(T_{m+N_2}^{n+1}+T_{m+N_2}^{n}\right)\right]+[\beta-2Dx-2Dy-2Dz]T_m^n\right]+S(m)\right\}}{(\beta+2Dx+2Dy+2Dz)} \quad (3.23)$$

H i=N_x, j=1, k=N_z

$$T_m^{n+1} = \frac{\left\{\left[\left[2Dx\left(T_{m-1}^{n+1}+T_{m-1}^{n}\right)+2Dy\left(T_{m+N_x}^{n+1}+T_{m+N_x}^{n}\right)+2Dz\left(T_{m-N_2}^{n+1}+T_{m-N_2}^{n}\right)\right]+[\beta-2Dx-2Dy-2Dz]T_m^n\right]+S(m)\right\}}{(\beta+2Dx+2Dy+2Dz)} \quad (3.24)$$

C i=N_x, j=N_y, k=1

$$T_m^{n+1} = \frac{\left\{\left[\left[2Dx\left(T_{m-1}^{n+1}+T_{m-1}^{n}\right)+2Dy\left(T_{m-N_x}^{n+1}+T_{m-N_x}^{n}\right)+2Dz\left(T_{m+N_2}^{n+1}+T_{m+N_2}^{n}\right)\right]+[\beta-2Dx-2Dy-2Dz]T_m^n\right]+S(m)\right\}}{(\beta+2Dx+2Dy+2Dz)} \quad (3.25)$$

G i=N_x, j=N_y, k=N_z

$$T_m^{n+1} = \frac{\left\{\left[\left[2Dx\left(T_{m-1}^{n+1}+T_{m-1}^{n}\right)+2Dy\left(T_{m-N_x}^{n+1}+T_{m-N_x}^{n}\right)+2Dz\left(T_{m-N_2}^{n+1}+T_{m-N_2}^{n}\right)\right]+[\beta-2Dx-2Dy-2Dz]T_m^n\right]+S(m)\right\}}{(\beta+2Dx+2Dy+2Dz)} \quad (3.26)$$

3.2.3.3 For the Lines

Line 1 i=2 :(Nx-1), j=1, k=1

$$T_m^{n+1} = \frac{\left\{\left[\left[Dx\left(T_{m+1}^{n+1}+T_{m-1}^{n+1}+T_{m+1}^{n}+T_{m-1}^{n}\right)+2Dy\left(T_{m+N_x}^{n+1}+T_{m+N_x}^{n}\right)+2Dz\left(T_{m+N_2}^{n+1}+T_{m+N_2}^{n}\right)\right]+[\beta-2Dx-2Dy-2Dz]T_m^n\right]+S(m)\right\}}{(\beta+2Dx+2Dy+2Dz)}$$

(3.27)

Line 6 i=N_x, j=1, k=2: (N_z-1)

$$T_m^{n+1} = \frac{\left\{\left[\left[2Dx\left(T_{m-1}^{n+1}+T_{m-1}^{n}\right)+2Dy\left(T_{m+N_x}^{n+1}+T_{m+N_x}^{n}\right)+Dz\left(T_{m+N_2}^{n+1}+T_{m-N_2}^{n+1}+T_{m+N_2}^{n}+T_{m-N_2}^{n}\right)\right]+[\beta-2Dx-2Dy-2Dz]T_m^n\right]+S(m)\right\}}{(\beta+2Dx+2Dy+2Dz)}$$

(3.28)

Line 9 i=2: (N_x-1), j=1, k=N_z

$$T_m^{n+1} = \frac{\left\{\left[\left[Dx\left(T_{m+1}^{n+1}+T_{m-1}^{n+1}+T_{m+1}^{n}+T_{m-1}^{n}\right)+2Dy\left(T_{m+N_x}^{n+1}+T_{m+N_x}^{n}\right)+2Dz\left(T_{m-N_2}^{n+1}+T_{m-N_2}^{n}\right)\right]+[\beta-2Dx-2Dy-2Dz]T_m^n\right]+S(m)\right\}}{(\beta+2Dx+2Dy+2Dz)} \quad (3.29)$$

Line 5 i=1, j=1, k=2: (N_z-1)

$$T_m^{n+1} = \frac{\left\{\left[\left[2Dx\left(T_{m+1}^{n+1}+T_{m+1}^{n}\right)+2Dy\left(T_{m+N_x}^{n+1}+T_{m+N_x}^{n}\right)+Dz\left(T_{m+N_2}^{n+1}+T_{m-N_2}^{n+1}+T_{m+N_2}^{n}+T_{m-N_2}^{n}\right)\right]+[\beta-2Dx-2Dy-2Dz]T_m^n\right]+S(m)\right\}}{(\beta+2Dx+2Dy+2Dz)} \quad (3.30)$$

Line 4 i=1, j=2: (N_y-1), k=1

$$T_m^{n+1} = \frac{\left\{\left[\left[2Dx\left(T_{m+1}^{n+1}+T_{m+1}^{n}\right)+Dy\left(T_{m+N_x}^{n+1}+T_{m-N_x}^{n+1}+T_{m+N_x}^{n}+T_{m-N_x}^{n}\right)+2Dz\left(T_{m+N_2}^{n+1}+T_{m+N_2}^{n}\right)\right]+[\beta-2Dx-2Dy-2Dz]T_m^n\right]+S(m)\right\}}{(\beta+2Dx+2Dy+2Dz)} \quad (3.31)$$

Line 2 i=N_x, j=2: (N_y-1), k=1

$$T_m^{n+1} = \frac{\left\{\left[\left[2Dx\left(T_{m-1}^{n+1}+T_{m-1}^{n}\right)+Dy\left(T_{m+N_x}^{n+1}+T_{m-N_x}^{n+1}+T_{m+N_x}^{n}+T_{m-N_x}^{n}\right)+2Dz\left(T_{m+N_2}^{n+1}+T_{m+N_2}^{n}\right)\right]+[\beta-2Dx-2Dy-2Dz]T_m^n\right]+S(m)\right\}}{(\beta+2Dx+2Dy+2Dz)} \quad (3.32)$$

Line 10 i=N_x, j=2: (N_y-1), k=N_z

$$T_m^{n+1} = \frac{\left\{\left[\left[2Dx\left(T_{m-1}^{n+1}+T_{m-1}^{n}\right)+Dy\left(T_{m+N_x}^{n+1}+T_{m-N_x}^{n+1}+T_{m+N_x}^{n}+T_{m-N_x}^{n}\right)+2Dz\left(T_{m-N_2}^{n+1}+T_{m-N_2}^{n}\right)\right]+[\beta-2Dx-2Dy-2Dz]T_m^n\right]+S(m)\right\}}{(\beta+2Dz+2Dy+2Dz)} \quad (3.33)$$

Line 12 i=1, j=2: (N_y-1), k=N_z

$$T_m^{n+1} = \frac{\left\{\left[\left[2Dx\left(T_{m+1}^{n+1}+T_{m+1}^{n}\right)+Dy\left(T_{m+N_x}^{n+1}+T_{m-N_x}^{n+1}+T_{m+N_x}^{n}+T_{m-N_x}^{n}\right)+2Dz\left(T_{m-N_2}^{n+1}+T_{m-N_2}^{n}\right)\right]+[\beta-2Dx-2Dy-2Dz]T_m^n\right]+S(m)\right\}}{(\beta+2Dx+2Dy+2Dz)} \quad (3.34)$$

Line 3 i=2: (N_x-1), j=N_y, k=1

$$T_m^{n+1} = \frac{\left\{\left[\left[Dx\left(T_{m+1}^{n+1}+T_{m-1}^{n+1}+T_{m+1}^{n}+T_{m-1}^{n}\right)+2Dy\left(T_{m-N_x}^{n+1}+T_{m-N_x}^{n}\right)+2Dz\left(T_{m+N_2}^{n+1}+T_{m+N_2}^{n}\right)\right]+[\beta-2Dx-2Dy-2Dz]T_m^n\right]+S(m)\right\}}{(\beta+2Dx+2Dy+2Dz)} \quad (3.35)$$

Line 7 i=N_x, j=N_y, k=2: (N_z-1)

$$T_m^{n+1} = \frac{\left\{\left[\left[2Dx\left(T_{m-1}^{n+1}+T_{m-1}^{n}\right)+2Dy\left(T_{m-N_x}^{n+1}+T_{m-N_x}^{n}\right)+Dz\left(T_{m+N_2}^{n+1}+T_{m-N_2}^{n+1}+T_{m+N_2}^{n}+T_{m-N_2}^{n}\right)\right]+[\beta-2Dx-2Dy-2Dz]T_m^n\right]+S(m)\right\}}{(\beta+2Dx+2Dy+2Dz)} \quad (3.36)$$

Line 11 i=2: (N_x-1), j=N_y, k=N_z

$$T_m^{n+1} = \frac{\left\{\left[\left[Dx\left(T_{m+1}^{n+1}+T_{m-1}^{n+1}+T_{m+1}^{n}+T_{m-1}^{n}\right)+2Dy\left(T_{m-N_x}^{n+1}+T_{m-N_x}^{n}\right)+2Dz\left(T_{m-N_2}^{n+1}+T_{m-N_2}^{n}\right)\right]+[\beta-2Dx-2Dy-2Dz]T_m^n\right]+S(m)\right\}}{(\beta+2Dx+2Dy+2Dz)} \quad (3.37)$$

Line 8 i=1, j=N_y, k=2: (N_z-1)

$$T_m^{n+1} = \frac{\left\{\left[\left[2Dx\left(T_{m+1}^{n+1}+T_{m+1}^{n}\right)+2Dy\left(T_{m-N_x}^{n+1}+T_{m-N_x}^{n}\right)+Dz\left(T_{m+N_2}^{n+1}+T_{m-N_2}^{n+1}+T_{m+N_2}^{n}+T_{m-N_2}^{n}\right)\right]+[\beta-2Dx-2Dy-2Dz]T_m^n\right]+S(m)\right\}}{(\beta+2Dx+2Dy+2Dz)} \quad (3.38)$$

3.2.3.4 For the faces,

Face 1 i=1, j=2: (N_y-1), k=2: (N_z-1)

$$T_m^{n+1} = \frac{\left\{\left[\left[2Dx\left(T_{m+1}^{n+1}+T_{m+1}^{n}\right)+Dy\left(T_{m+N_x}^{n+1}+T_{m-N_x}^{n+1}+T_{m+N_x}^{n}+T_{m-N_x}^{n}\right)+Dz\left(T_{m+N_2}^{n+1}+T_{m-N_2}^{n+1}+T_{m+N_2}^{n}+T_{m-N_2}^{n}\right)\right]+[\beta-2Dx-2Dy-2Dz]T_m^n\right]+S(m)\right\}}{(\beta+2Dx+2Dy+2Dz)}$$

(3.39)

Face 2 i=N_x, j=2: (N_y-1), k=2: (N_z-1)

$$T_m^{n+1} = \frac{\left\{\left[\left[2Dx\left(T_{m-1}^{n+1}+T_{m-1}^{n}\right)+Dy\left(T_{m+N_x}^{n+1}+T_{m-N_x}^{n+1}+T_{m+N_x}^{n}+T_{m-N_x}^{n}\right)+Dz\left(T_{m+N_2}^{n+1}+T_{m-N_2}^{n+1}+T_{m+N_2}^{n}+T_{m-N_2}^{n}\right)\right]+[\beta-2Dx-2Dy-2Dz]T_m^n\right]+S(m)\right\}}{(\beta+2Dx+2Dy+2Dz)}$$

(3.40)

Face 5 i= 2: (N_x-1), j=1, k=2: (N_z-1)

$$T_m^{n+1} = \frac{\left\{\left[\left[Dx\left(T_{m+1}^{n+1}+T_{m-1}^{n+1}+T_{m+1}^{n}+T_{m-1}^{n}\right)+2Dy\left(T_{m+N_x}^{n+1}+T_{m+N_x}^{n}\right)+Dz\left(T_{m+N_2}^{n+1}+T_{m-N_2}^{n+1}+T_{m+N_2}^{n}+T_{m-N_2}^{n}\right)\right]+[\beta-2Dx-2Dy-2Dz]T_m^n\right]+S(m)\right\}}{(\beta+2Dx+2Dy+2Dz)}$$

(3.41)

Face 6 i=2: (N_x-1), j=N_y, k=2: (N_z-1)

$$T_m^{n+1} = \frac{\left\{\left[\left[Dx\left(T_{m+1}^{n+1}+T_{m-1}^{n+1}+T_{m+1}^{n}+T_{m-1}^{n}\right)+2Dy\left(T_{m-N_x}^{n+1}+T_{m-N_x}^{n}\right)+Dz\left(T_{m+N_2}^{n+1}+T_{m-N_2}^{n+1}+T_{m+N_2}^{n}+T_{m-N_2}^{n}\right)\right]+[\beta-2Dx-2Dy-2Dz]T_m^n\right]+S(m)\right\}}{(\beta+2Dx+2Dy+2Dz)}$$

(3.42)

Face 3 i=2: (Nx-1), j=2: (Ny-1), k=1

$$T_m^{n+1} = \frac{\left\{\left[\left[Dx\left(T_{m+1}^{n+1}+T_{m-1}^{n+1}+T_{m+1}^{n}+T_{m-1}^{n}\right)+Dy\left(T_{m+N_x}^{n+1}+T_{m-N_x}^{n+1}+T_{m+N_x}^{n}+T_{m-N_x}^{n}\right)+2Dz\left(T_{m+N_2}^{n+1}+T_{m+N_2}^{n}\right)\right]+[\beta-2Dx-2Dy-2Dz]T_m^n\right]+S(m)\right\}}{(\beta+2Dx+2Dy+2Dz)}$$

(3.43)

Face 4 i=2: (Nx-1), j=2: (Ny-1), k=Nz

$$T_m^{n+1} = \frac{\left\{\left[\left[2Dx\left(T_{m+1}^{n+1}+T_{m-1}^{n+1}+T_{m+1}^{n}+T_{m-1}^{n}\right)+Dy\left(T_{m+N_x}^{n+1}+T_{m-N_x}^{n+1}+T_{m+N_x}^{n}+T_{m-N_x}^{n}\right)+2Dz\left(T_{m-N_2}^{n+1}+T_{m-N_2}^{n}\right)\right]+[\beta-2Dx-2Dy-2Dz]T_m^n\right]+S(m)\right\}}{(\beta+2Dx+2Dy+2Dz)}$$

(3.44)

3.3 Viscosity Correlation

One of the major mechanisms of oil recovery by thermal processes is viscosity reduction of oil as temperature increased. By reducing the oil viscosity, a higher mobility is developed thus the fluid flows much easier.

Using Braden formula for oils (Marcel et al. 1980),

$$\log(v_2 + C) = \left[\frac{T_1}{T_2}\right]^D log(v_1 + C) \quad (3.45)$$

Where C is a constant (equals 0.6 if v > 1.5cst)

D is a constant of the order of 3.5 to 4

v is the kinematic viscosity in centistokes. Assuming 1 centistoke = 1 centipoise.

T is the absolute temperature.

The temperature known from the heat model are coupled with the viscosity correlation to know how temperature affect viscosity.

3.4 Pressure Model

The pressure model is to be coupled with the generated viscosity values.

3.4.1 Mathematical Model

The model is developed using Navier Stokes' equation with a horizontal well serving as a sink and inculcating the appropriate initial and boundary conditions that represents the performance of the reservoir. The model is basically governed by

1. Law of mass conservation,
2. Darcy's Law (transport equation), and
3. Equation of state (phase properties such as density, compressibility and formation volume factor).

Basic Assumptions

- Homogeneous and Anisotropic reservoir
- Single-phase and slightly compressible fluid
- Negligible gravity effect
- Transient effective viscosity

- Uniform grid size
- Constant compressibility above bubble point pressure
- No-flow reservoir boundary condition
- Constant permeability, porosity and compressibility
- Varying formation volume factor dependent on pressure
- Horizontal Well

3.4.1.1 Derivation of the diffusivity Equation

$$(Total\ mass\ entering\ CV\ during\ \Delta t) - (Total\ mass\ leaving\ CV\ during\ \Delta t\ )$$

$$= (Net\ change\ in\ mass\ within\ CV during\ \Delta t)$$

i.e. $M_{in} - M_{out} = \Delta M_v$ (3.46)

$$M_{in} = \left(\dot{m}\big|_x + \dot{m}\big|_y + \dot{m}\big|_z\right)\Delta t \quad (3.46a)$$

$$M_{out} = \left(\dot{m}\big|_{x+\Delta x} + \dot{m}\big|_{y+\Delta y} + \dot{m}\big|_{z+\Delta z} + q_s\right)\Delta t \quad (3.46b)$$

$$\Delta M_v = \left(M_v\emptyset\big|_{t+\Delta t} - M_v\emptyset\big|_t\right) \quad (3.46c)$$

Combining equations (3.46a), (3.46b) and (3.46c) to get

$$\left(\dot{m}\big|_x + \dot{m}\big|_y + \dot{m}\big|_z\right)\Delta t - \left(\dot{m}\big|_{x+\Delta x} + \dot{m}\big|_{y+\Delta y} + \dot{m}\big|_{z+\Delta z} + q_s\right)\Delta t = \left(M_v\emptyset\big|_{t+\Delta t} - M_v\emptyset\big|_t\right) \quad (3.47)$$

Where $\dot{m}$ = mass flow rate,

ρ = density,

Φ = porosity,

u = velocity,

A = cross sectional area

q_s = mass flow rate (sink term) of production

$$\dot{m} = \rho u A \tag{3.47a}$$

$$M_v = \rho V_b \tag{3.47b}$$

Substituting equations (3.47a) and (3.47b) into (3.47), dividing through V_b and rearranging it to get

$$-\left\{\left[\frac{\rho u_x|_{x+\Delta x}-\rho u_x|_x}{\Delta x}\right]+\left[\frac{\rho u_y|_{y+\Delta y}-\rho u_y|_y}{\Delta y}\right]+\left[\frac{\rho u_z|_{z+\Delta z}-\rho u_z|_z}{\Delta z}\right]+\frac{q_s}{V_b}\right\}=\left\{\frac{\rho\emptyset|_{t+\Delta t}-\rho\emptyset|_t}{\Delta t}\right\} \tag{3.48}$$

Taking limit as $\Delta x \to 0$, $\Delta y \to 0$, $\Delta z \to 0$ and $\Delta t = 0$ to give:

$$-\left\{\frac{\partial(\rho u_x)}{\partial x}+\frac{\partial(\rho u_y)}{\partial y}+\frac{\partial(\rho u_z)}{\partial z}+\frac{q_s}{V_b}\right\}=\frac{\partial(\rho\emptyset)}{\partial t} \tag{3.49}$$

From Darcy's Law,

$$u = -\beta_c \frac{k}{\mu}(\nabla P - \gamma \nabla Z) \tag{3.49a}$$

From the equation of state,

$$B_o = \frac{V_b}{V_{sc}} = \frac{\rho_{sc}}{\rho} \tag{3.49b}$$

$$q_s = \alpha_c \rho q \tag{3.49c}$$

Where α_c = volume conversion factor (to field unit) = 5.615

β_c =unit conversion factor for permeability coefficient = 1.127

k = rock permeability (md)

ρ_{sc} = density at surface condition

ρ = density at reservoir condition

V_{sc} = volume at surface condition (stb)

Vb = volume at reservoir condition (rb)

μ = dynamic viscosity of the fluid (cp)

P = pressure (psia)

Z = elevation (ft)

γ = fluid gravity (psi/ft)

B_o = oil formation volume factor (rb/stb)

q = volumetric flow rate of production (stb/D)

Using equations (3.49a), (3.49b), (3.49c), dividing through by $\alpha_c\rho_{sc}$ and multiplying through by V_b, assuming negligible gravity effect,

$$\frac{\partial}{\partial x}\left(\beta_c \frac{A_x k_x}{\mu B_o}\frac{\partial P}{\partial x}\right)\Delta x + \frac{\partial}{\partial y}\left(\beta_c \frac{A_y k_y}{\mu B_o}\frac{\partial P}{\partial y}\right)\Delta y + \frac{\partial}{\partial z}\left(\beta_c \frac{A_z k_z}{\mu B_o}\frac{\partial P}{\partial z}\right)\Delta z - q = \frac{V_b}{\alpha_c}\frac{\partial}{\partial t}\left(\frac{\emptyset}{B_o}\right) \qquad (3.50$$

3.4.2 Numerical model

The equation for the mathematical model is complex to be solved by analytical method thus the finite difference method is used to put the equation in a form that is solvable by digital computer. This process involves spatial and time derivative discretization. The general PDE for a single phase three dimensional flow through porous medium may be written in Cartesian coordinates as:

$$\frac{\partial}{\partial x}\left(\beta_c \frac{A_x k_x}{\mu B_o}\frac{\partial P}{\partial x}\right)\Delta x + \frac{\partial}{\partial y}\left(\beta_c \frac{A_y k_y}{\mu B_o}\frac{\partial P}{\partial y}\right)\Delta y + \frac{\partial}{\partial z}\left(\beta_c \frac{A_z k_z}{\mu B_o}\frac{\partial P}{\partial z}\right)\Delta z - q = \frac{V_b \emptyset C_t}{\alpha_c B_o}\frac{\partial P}{\partial t} \qquad (3.51)$$

Where C_t = total compressibility

3.4.2.1 Spatial Discretization

Using Central difference scheme, to discretize the left hand side of the equation (3.51) along the three orthogonal directions is shown below;

For the x direction

$$\text{Let } a = \beta_c \frac{A_x}{\mu} \frac{k_x}{B_o} \tag{3.51a}$$

$$P' = \frac{\partial P}{\partial x} \tag{3.51b}$$

$$F(x) = aP' \tag{3.51c}$$

$$\frac{\partial}{\partial x}\left(\beta_c \frac{A_x k_x}{\mu B_o}\frac{\partial P}{\partial x}\right)_{i,j,k} \approx \frac{\partial F}{\partial x} \approx \frac{F_{i+1/2,j,k} - F_{i-1/2,j,k}}{\Delta x} \approx \frac{(aP')_{i+1/2,j,k} - (aP')_{i-1/2,j,k}}{\Delta x} \tag{3.52}$$

$$(aP')_{i+1/2,j,k} \approx a_{i+1/2,j,k} P'_{i+1/2,j,k} \approx a_{i+1/2,j,k} \frac{P_{i+1,j,k} - P_{i,j,k}}{\Delta x}$$

$$(aP')_{i-1/2,j,k} \approx a_{i-1/2,j,k} P'_{i-1/2,j,k} \approx a_{i-1/2,j,k} \frac{P_{i,j,k} - P_{i-1,j,k}}{\Delta x}$$

Thus equation (3.48) becomes:

$$\approx \frac{a_{i+1/2,j,k}\frac{P_{i+1,j,k} - P_{i,j,k}}{\Delta x} - a_{i-1/2,j,k}\frac{P_{i,j,k} - P_{i-1,j,k}}{\Delta x}}{\Delta x} \approx \frac{a_{i+1/2,j,k}(P_{i+1,j,k} - P_{i,j,k}) - a_{i-1/2,j,k}(P_{i,j,k} - P_{i-1,j,k})}{(\Delta x)^2} \tag{3.53}$$

Similarly along the y direction,

$$\frac{\partial}{\partial y}\left(\beta_c \frac{A_y k_y}{\mu B_o}\frac{\partial P}{\partial y}\right)_{i,j,k} \approx \frac{a_{i,j+1/2,k}(P_{i,j+1,k} - P_{i,j,k}) - a_{i,j-1/2,k}(P_{i,j,k} - P_{i,j-1,k})}{(\Delta y)^2} \tag{3.54}$$

Similarly along the z direction,

$$\frac{\partial}{\partial z}\left(\beta_c \frac{A_z k_z}{\mu B_o}\frac{\partial P}{\partial z}\right)_{i,j,k} \approx \frac{a_{i,j,k+1/2}(P_{i,j,k+1}-P_{i,j,k})-a_{i,j,k-1/2}(P_{i,j,k}-P_{i,j,k-1})}{(\Delta z)^2} \quad (3.55)$$

Substituting Equations (3.53), (3.54) and (3.55) into (3.51) to obtain:

$$\frac{a_{i+1/2,j,k}(P_{i+1,j,k}-P_{i,j,k})-a_{i-1/2,j,k}(P_{i,j,k}-P_{i-1,j,k})}{(\Delta x)^2}\Delta x + \frac{a_{i,j+1/2,k}(P_{i,j+1,k}-P_{i,j,k})-a_{i,j-1/2,k}(P_{i,j,k}-P_{i,j-1,k})}{(\Delta y)^2}\Delta y +$$

$$\frac{a_{i,j,k+1/2}(P_{i,j,k+1}-P_{i,j,k})-a_{i,j,k-1/2}(P_{i,j,k}-P_{i,j,k-1})}{(\Delta z)^2}\Delta z - q = \frac{V_b \emptyset C_t}{\alpha_c B_o}\frac{\partial P}{\partial t}$$

If $A_{i\pm1/2,j,k} = \frac{a_{i\pm1/2,j,k}}{\Delta x}$

Thus

$$A_{i+1/2,j,k}(P_{i+1,j,k}-P_{i,j,k}) - A_{i-1/2,j,k}(P_{i,j,k}-P_{i-1,j,k}) + A_{i,j+1/2,k}(P_{i,j+1,k}-P_{i,j,k}) - A_{i,j-1/2,k}(P_{i,j,k}-P_{i,j-1,k}) +$$

$$A_{i,j,k+1/2}(P_{i,j,k+1}-P_{i,j,k}) - A_{i,j,k-1/2}(P_{i,j,k}-P_{i,j,k-1}) - q_{i,j,k} = \left(\frac{V_b \emptyset C_t}{\alpha_c B_o}\right)_{i,j,k}\left(\frac{\partial P}{\partial t}\right)_{i,j,k} \quad (3.56)$$

3.4.2.2 Time Discretization

Using the backward difference for discretizing the time derivative with a base time level n+1;

$$\left(\frac{V_b \emptyset C_t}{\alpha_c B_o}\right)_{i,j,k}\left(\frac{\partial P}{\partial t}\right)_{i,j,k} = \left(\frac{V_b \emptyset C_t}{\alpha_c B_o \Delta t}\right)_{i,j,k}\left(P_{i,j,k}^{n+1} - P_{i,j,k}^{n}\right) = \gamma_{i,j,k}\left(P_{i,j,k}^{n+1} - P_{i,j,k}^{n}\right) \quad (3.57)$$

Where $\gamma_{i,j,k} = \left(\frac{V_b \emptyset C_t}{\alpha_c B_o \Delta t}\right)_{i,j,k}$

In order to obtain an unconditionally stable scheme, Crank Nicolson scheme is employed for equation (3.56) while substituting (3.57) into it.

$$\gamma_{i,j,k}\left(P_{i,j,k}^{n+1} - P_{i,j,k}^{n}\right) = \frac{1}{2}\left\{\left(A_{i+1/2,j,k}^{n+1}\left(P_{i+1,j,k}^{n+1} - P_{i,j,k}^{n+1}\right) - A_{i-1/2,j,k}^{n+1}\left(P_{i,j,k}^{n+1} - P_{i-1,j,k}^{n+1}\right) + A_{i,j+1/2,k}^{n+1}\left(P_{i,j+1,k}^{n+1} - P_{i,j,k}^{n+1}\right) -\right.\right.$$

$$A_{i,j-1/2,k}^{n+1}\left(P_{i,j,k}^{n+1} - P_{i,j-1,k}^{n+1}\right) + A_{i,j,k+1/2}^{n+1}\left(P_{i,j,k+1}^{n+1} - P_{i,j,k}^{n+1}\right) - A_{i,j,k-1/2}^{n+1}\left(P_{i,j,k}^{n+1} - P_{i,j,k-1}^{n+1}\right)\Big) + \Big(A_{i+1/2,j,k}^{n}\left(P_{i+1,j,k}^{n} - P_{i,j,k}^{n}\right) -$$

$$A_{i-1/2,j,k}^{n}\left(P_{i,j,k}^{n} - P_{i-1,j,k}^{n}\right) + A_{i,j+1/2,k}^{n}\left(P_{i,j+1,k}^{n} - P_{i,j,k}^{n}\right) - A_{i,j-1/2,k}^{n}\left(P_{i,j,k}^{n} - P_{i,j-1,k}^{n}\right) + A_{i,j,k+1/2}^{n}\left(P_{i,j,k+1}^{n} - P_{i,j,k}^{n}\right) -$$

$$\left.\left.A_{i,j,k-1/2}^{n}\left(P_{i,j,k}^{n} - P_{i,j,k-1}^{n}\right)\Big)\right\} - q_{i,j,k} \quad (3.58)$$

3.4.3 Computer Model (Matlab Programming)

Using Figure 3.1, the numerical model obtained for the three-dimensional oil reservoir (3.58) requires high speed digital computer due to the large amount of calculation. Below are the linear equations generated as a result of the boundary condition for the reservoir.

Using equations (3.14c), (3.14d), (3.14e), (3.14f), (3.14g) and (3.14h),

Let $A^{n+1}_{i+1/2,j,k} = 0.5\left(A^{n+1}_{i,j,k} + A^{n+1}_{i+1,j,k}\right) = 0.5(A^{n+1}_{m} + A^{n+1}_{m+1}) = \text{temp1b}$ (3.58a)

$$A^{n+1}_{i-1/2,j,k} = 0.5\left(A^{n+1}_{i,j,k} + A^{n+1}_{i-1,j,k}\right) = 0.5(A^{n+1}_{m} + A^{n+1}_{m-1}) = \text{temp2b} \quad (3.58b)$$

$$A^{n+1}_{i,j+1/2,k} = 0.5\left(A^{n+1}_{i,j,k} + A^{n+1}_{i,j+1,k}\right) = 0.5\left(A^{n+1}_{m} + A^{n+1}_{m+N_x}\right) = \text{temp3b} \quad (3.58c)$$

$$A^{n+1}_{i,j-1/2,k} = 0.5\left(A^{n+1}_{i,j,k} + A^{n+1}_{i,j-1,k}\right) = 0.5\left(A^{n+1}_{m} + A^{n+1}_{m-N_x}\right) = \text{temp4b} \quad (3.58d)$$

$$A^{n+1}_{i,j,k+1/2} = 0.5\left(A^{n+1}_{i,j,k} + A^{n+1}_{i,j,k+1}\right) = 0.5\left(A^{n+1}_{m} + A^{n+1}_{m+N_2}\right) = \text{temp5b} \quad (3.58e)$$

$$A^{n+1}_{i,j,k-1/2} = 0.5\left(A^{n+1}_{i,j,k} + A^{n+1}_{i,j,k-1}\right) = 0.5\left(A^{n+1}_{m} + A^{n+1}_{m-N_2}\right) = \text{temp6b} \quad (3.58f)$$

$$A^{n}_{i+1/2,j,k} = 0.5\left(A^{n}_{i,j,k} + A^{n}_{i+1,j,k}\right) = 0.5(A^{n}_{m} + A^{n}_{m+1}) = \text{temp1} \quad (3.58g)$$

$$A^{n}_{i-1/2,j,k} = 0.5\left(A^{n}_{i,j,k} + A^{n}_{i-1,j,k}\right) = 0.5(A^{n}_{m} + A^{n}_{m-1}) = \text{temp2} \quad (3.58h)$$

$$A^{n}_{i,j+1/2,k} = 0.5\left(A^{n}_{i,j,k} + A^{n}_{i,j+1,k}\right) = 0.5\left(A^{n}_{m} + A^{n}_{m+N_x}\right) = \text{temp3} \quad (3.58i)$$

$$A^{n}_{i,j-1/2,k} = 0.5\left(A^{n}_{i,j,k} + A^{n}_{i,j-1,k}\right) = 0.5\left(A^{n}_{m} + A^{n}_{m-N_x}\right) = \text{temp4} \quad (3.58j)$$

$$A^{n}_{i,j,k+1/2} = 0.5\left(A^{n}_{i,j,k} + A^{n}_{i,j,k+1}\right) = 0.5\left(A^{n}_{m} + A^{n}_{m+N_2}\right) = \text{temp5} \quad (3.58k)$$

$$A^{n}_{i,j,k-1/2} = 0.5\left(A^{n}_{i,j,k} + A^{n}_{i,j,k-1}\right) = 0.5\left(A^{n}_{m} + A^{n}_{m-N_2}\right) = \text{temp6} \quad (3.58l)$$

$$\beta = 2\gamma \quad (3.58m)$$

Applying no flow boundary conditions:

$$\frac{\partial P}{\partial x} = 0 \tag{3.59}$$

$$\frac{P_{x+\Delta x} - P_{x-\Delta x}}{2\Delta x} = 0 \rightarrow \ P_{x+\Delta x} = P_{x-\Delta x}$$

$$\frac{\partial P}{\partial x} \rightarrow P_{m+1} = P_{m-1} \tag{3.60}$$

$$\frac{\partial P}{\partial y} \rightarrow P_{m+N_x} = P_{m-N_x} \tag{3.61}$$

$$\frac{\partial P}{\partial z} \rightarrow P_{m+N_2} = P_{m-N_2} \tag{3.62}$$

3.4.3.1 For interior nodes

$\beta(P_m^{n+1} - P_m^n) = \{(temp1b(P_{m+1}^{n+1} - P_m^{n+1}) - temp2b(P_m^{n+1} - P_{m-1}^{n+1}) + temp3b(P_{m+N_x}^{n+1} - P_m^{n+1}) - temp4b(P_m^{n+1} - P_{m-N_x}^{n+1}) + temp5b(P_{m+N_2}^{n+1} - P_m^{n+1}) - temp6b(P_m^{n+1} - P_{m-N_2}^{n+1})) + (temp1(P_{m+1}^n - P_m^n) - temp2(P_m^n - P_{m-1}^n) + temp3(P_{m+N_x}^n - P_m^n) - temp4(P_m^n - P_{m-N_x}^n) + temp5(P_{m+N_2}^n - P_m^n) - temp6(P_m^n - P_{m-N_2}^n))\} - 2q_{i,j,k}$

$(\beta + temp1b + temp2b + temp3b + temp4b + temp5b + temp6b)P_m^{n+1} = \{(temp1bP_{m+1}^{n+1} + temp2bP_{m-1}^{n+1} + temp3bP_{m+N_x}^{n+1} + temp4bP_{m-N_x}^{n+1} + temp5bP_{m+N_2}^{n+1} - temp6bP_{m-N_2}^{n+1}) + (temp1P_{m+1}^n + temp2P_{m-1}^n + temp3P_{m+N_x}^n + temp4P_{m-N_x}^n + temp5P_{m+N_2}^n + temp6P_{m-N_2}^n) - (temp1 + temp2 + temp3 + temp4 + temp5 + temp6 - \beta)P_m^n\} - 2q_{i,j,k}$

Rearranging the equation;

$P_m^{n+1} = \{(temp1bP_{m+1}^{n+1} + temp2bP_{m-1}^{n+1} + temp3bP_{m+N_x}^{n+1} + temp4bP_{m-N_x}^{n+1} + temp5bP_{m+N_2}^{n+1} + temp6bP_{m-N_2}^{n+1}) + (temp1P_{m+1}^n + temp2P_{m-1}^n + temp3P_{m+N_x}^n + temp4P_{m-N_x}^n + temp5P_{m+N_2}^n + temp6P_{m-N_2}^n) - (temp1 + temp2 + temp3 + temp4 + temp5 + temp6 - \beta)P_m^n - S(m)\}/(\beta + temp1b + temp2b + temp3b + temp4b + temp5b + temp6b)$ (3.63)

Special Points

There are 26 special points which are treated differently due to the no flow boundary condition and these include 6 faces, 8 corners and 12 lines.

3.4.3.2 For the corners,

A i=1, j=1, k=1

$$P_m^{n+1} = \Big\{\Big((temp1b + temp2b)P_{m+1}^{n+1} + (temp3b + temp4b)P_{m+N_x}^{n+1} + (temp5b + temp6b)P_{m+N_2}^{n+1}\Big) + \Big((temp1 + temp2)P_{m+1}^{n} + (temp3 + temp4)P_{m+N_x}^{n} + (temp5 + temp6)P_{m+N_2}^{n}\Big) - (temp1 + temp2 + temp3 + temp4 + temp5 + temp6 - \beta)P_m^n - S(m)\Big\}/(\beta + temp1b + temp2b + temp3b + temp4b + temp5b + temp6b) \quad (3.64)$$

E i=1, j=1, k= N_z

$$P_m^{n+1} = \Big\{\Big((temp1b + temp2b)P_{m+1}^{n+1} + (temp3b + temp4b)P_{m+N_x}^{n+1} + (temp5b + temp6b)P_{m-N_2}^{n+1}\Big) + \Big((temp1 + temp2)P_{m+1}^{n} + (temp3 + temp4)P_{m+N_x}^{n} + (temp5 + temp6)P_{m-N_2}^{n}\Big) - (temp1 + temp2 + temp3 + temp4 + temp5 + temp6 - \beta)P_m^n - S(m)\Big\}/(\beta + temp1b + temp2b + temp3b + temp4b + temp5b + temp6b) \quad (3.65)$$

D i=1, j=N_y, k=1

$$P_m^{n+1} = \Big\{\Big((temp1b + temp2b)P_{m+1}^{n+1} + (temp3b + temp4b)P_{m-N_x}^{n+1} + (temp5b + temp6b)P_{m+N_2}^{n+1}\Big) + \Big((temp1 + temp2)P_{m+1}^{n} + (temp3 + temp4)P_{m-N_x}^{n} + (temp5 + temp6)P_{m+N_2}^{n}\Big) - (temp1 + temp2 + temp3 + temp4 + temp5 + temp6 - \beta)P_m^n - S(m)\Big\}/(\beta + temp1b + temp2b + temp3b + temp4b + temp5b + temp6b) \quad (3.66)$$

F i=1, j=N_y, k=N_z

$$P_m^{n+1} = \Big\{\Big((temp1b + temp2b)P_{m+1}^{n+1} + (temp3b + temp4b)P_{m-N_x}^{n+1} + (temp5b + temp6b)P_{m-N_2}^{n+1}\Big) + \Big((temp1 + temp2)P_{m+1}^{n} + (temp3 + temp4)P_{m-N_x}^{n} + (temp5 + temp6)P_{m-N_2}^{n}\Big) - (temp1 + temp2 + temp3 + temp4 + temp5 + temp6 - \beta)P_m^n - S(m)\Big\}/(\beta + temp1b + temp2b + temp3b + temp4b + temp5b + temp6b) \quad (3.67)$$

B $i=N_x, j=1, k=1$

$$P_m^{n+1} = \left\{\left((temp1b + temp2b)P_{m-1}^{n+1} + (temp3b + temp4b)P_{m+N_x}^{n+1} + (temp5b + temp6b)P_{m+N_2}^{n+1}\right) + \left((temp1 + temp2)P_{m-1}^{n} + (temp3 + temp4)P_{m+N_x}^{n} + (temp5 + temp6)P_{m+N_2}^{n}\right) - (temp1 + temp2 + temp3 + temp4 + temp5 + temp6 - \beta)P_m^n - S(m)\right\}/(\beta + temp1b + temp2b + temp3b + temp4b + temp5b + temp6b) \quad (3.68)$$

H $i=N_x, j=1, k=N_z$

$$P_m^{n+1} = \left\{\left((temp1b + temp2b)P_{m-1}^{n+1} + (temp3b + temp4b)P_{m+N_x}^{n+1} + (temp5b + temp6b)P_{m-N_2}^{n+1}\right) + \left((temp1 + temp2)P_{m-1}^{n} + (temp3 + temp4)P_{m+N_x}^{n} + (temp5 + temp6)P_{m-N_2}^{n}\right) - (temp1 + temp2 + temp3 + temp4 + temp5 + temp6 - \beta)P_m^n - S(m)\right\}/(\beta + temp1b + temp2b + temp3b + temp4b + temp5b + temp6b) \quad (3.69)$$

C $i=N_x, j=N_y, k=1$

$$P_m^{n+1} = \left\{\left((temp1b + temp2b)P_{m-1}^{n+1} + (temp3b + temp4b)P_{m-N_x}^{n+1} + (temp5b + temp6b)P_{m+N_2}^{n+1}\right) + \left((temp1 + temp2)P_{m-1}^{n} + (temp3 + temp4)P_{m-N_x}^{n} + (temp5 + temp6)P_{m+N_2}^{n}\right) - (temp1 + temp2 + temp3 + temp4 + temp5 + temp6 - \beta)P_m^n - S(m)\right\}/(\beta + temp1b + temp2b + temp3b + temp4b + temp5b + temp6b) \quad (3.70)$$

G $i=N_x, j=N_y, k=N_z$

$$P_m^{n+1} = \left\{\left((temp1b + temp2b)P_{m-1}^{n+1} + (temp3b + temp4b)P_{m-N_x}^{n+1} + (temp5b + temp6b)P_{m-N_2}^{n+1}\right) + \left((temp1 + temp2)P_{m-1}^{n} + (temp3 + temp4)P_{m-N_x}^{n} + (temp5 + temp6)P_{m-N_2}^{n}\right) - (temp1 + temp2 + temp3 + temp4 + temp5 + temp6 - \beta)P_m^n - S(m)\right\}/(\beta + temp1b + temp2b + temp3b + temp4b + temp5b + temp6b) \quad (3.71)$$

3.4.3.3 For the Lines

Line 1 i=2 :(Nx-1), j=1, k=1

$$P_m^{n+1} = \{(temp1b P_{m+1}^{n+1} + temp2b P_{m-1}^{n+1} + (temp3b + temp4b) P_{m+N_x}^{n+1} + (temp5b + temp6b) P_{m+N_2}^{n+1}) + (temp1 P_{m+1}^{n} + temp2 P_{m-1}^{n} + (temp3 + temp4) P_{m+N_x}^{n} + (temp5 + temp6) P_{m+N_2}^{n}) - (temp1 + temp2 + temp3 + temp4 + temp5 + temp6 - \beta) P_m^n - S(m)\}/(\beta + temp1b + temp2b + temp3b + temp4b + temp5b + temp6b) \quad (3.72)$$

Line 6 i=N_x, j=1, k=2: (N_z-1)

$$P_m^{n+1} = \{((temp1b + temp2b) P_{m-1}^{n+1} + (temp3b + temp4b) P_{m+N_x}^{n+1} + temp5b P_{m+N_2}^{n+1} + temp6b P_{m-N_2}^{n+1}) + ((temp1 + temp2) P_{m-1}^{n} + (temp3 + temp4) P_{m+N_x}^{n} + temp5 P_{m+N_2}^{n} + temp6 P_{m-N_2}^{n}) - (temp1 + temp2 + temp3 + temp4 + temp5 + temp6 - \beta) P_m^n - S(m)\}/(\beta + temp1b + temp2b + temp3b + temp4b + temp5b + temp6b) \quad (3.73)$$

Line 9 i=2: (N_x-1), j=1, k=N_z

$$P_m^{n+1} = \{(temp1b P_{m+1}^{n+1} + temp2b P_{m-1}^{n+1} + (temp3b + temp4b) P_{m+N_x}^{n+1} + (temp5b + temp6b) P_{m-N_2}^{n+1}) + (temp1 P_{m+1}^{n} + temp2 P_{m-1}^{n} + (temp3 + temp4) P_{m+N_x}^{n} + (temp5 + temp6) P_{m-N_2}^{n}) - (temp1 + temp2 + temp3 + temp4 + temp5 + temp6 - \beta) P_m^n - S(m)\}/(\beta + temp1b + temp2b + temp3b + temp4b + temp5b + temp6b) \quad (3.74)$$

Line 5 i=1, j=1, k=2: (N_z-1)

$$P_m^{n+1} = \{((temp1b + temp2b) P_{m+1}^{n+1} + (temp3b + temp4b) P_{m+N_x}^{n+1} + temp5b P_{m+N_2}^{n+1} + temp6b P_{m-N_2}^{n+1}) + ((temp1 + temp2) P_{m+1}^{n} + (temp3 + temp4) P_{m+N_x}^{n} + temp5 P_{m+N_2}^{n} + temp6 P_{m-N_2}^{n}) - (temp1 + temp2 + temp3 + temp4 + temp5 + temp6 - \beta) P_m^n - S(m)\}/(\beta + temp1b + temp2b + temp3b + temp4b + temp5b + temp6b) \quad (3.75)$$

Line 4 i=1, j=2: (N_y-1), k=1

$$P_m^{n+1} = \left\{\left((temp1b + temp2b)P_{m+1}^{n+1} + temp3bP_{m+N_x}^{n+1} + temp4bP_{m-N_x}^{n+1} + (temp5b + temp6b)P_{m+N_2}^{n+1}\right) + \left((temp1 + temp2)P_{m+1}^{n} + temp3P_{m+N_x}^{n} + temp4P_{m-N_x}^{n} + (temp5 + temp6)P_{m+N_2}^{n}\right) - (temp1 + temp2 + temp3 + temp4 + temp5 + temp6 - \beta)P_m^n - S(m)\right\} / (\beta + temp1b + temp2b + temp3b + temp4b + temp5b + temp6b) \quad (3.76)$$

Line 2 i=N_x, j=2: (N_y-1), k=1

$$P_m^{n+1} = \left\{\left((temp1b + temp2b)P_{m-1}^{n+1} + temp3bP_{m+N_x}^{n+1} + temp4bP_{m-N_x}^{n+1} + (temp5b + temp6b)P_{m+N_2}^{n+1}\right) + \left((temp1 + temp2)P_{m-1}^{n} + temp3P_{m+N_x}^{n} + temp4P_{m-N_x}^{n} + (temp5 + temp6)P_{m+N_2}^{n}\right) - (temp1 + temp2 + temp3 + temp4 + temp5 + temp6 - \beta)P_m^n - S(m)\right\} / (\beta + temp1b + temp2b + temp3b + temp4b + temp5b + temp6b) \quad (3.77)$$

Line 10 i=N_x, j=2: (N_y-1), k=N_z

$$P_m^{n+1} = \left\{\left((temp1b + temp2b)P_{m-1}^{n+1} + temp3bP_{m+N_x}^{n+1} + temp4bP_{m-N_x}^{n+1} + (temp5b + temp6b)P_{m-N_2}^{n+1}\right) + \left((temp1 + temp2)P_{m-1}^{n} + temp3P_{m+N_x}^{n} + temp4P_{m-N_x}^{n} + (temp5 + temp6)P_{m-N_2}^{n}\right) - (temp1 + temp2 + temp3 + temp4 + temp5 + temp6 - \beta)P_m^n - S(m)\right\} / (\beta + temp1b + temp2b + temp3b + temp4b + temp5b + temp6b) \quad (3.78)$$

Line 12 i=1, j=2: (N_y-1), k=N_z

$$P_m^{n+1} = \left\{\left((temp1b + temp2b)P_{m+1}^{n+1} + temp3bP_{m+N_x}^{n+1} + temp4bP_{m-N_x}^{n+1} + (temp5b + temp6b)P_{m-N_2}^{n+1}\right) + \left((temp1 + temp2)P_{m+1}^{n} + temp3P_{m+N_x}^{n} + temp4P_{m-N_x}^{n} + (temp5 + temp6)P_{m-N_2}^{n}\right) - (temp1 + temp2 + temp3 + temp4 + temp5 + temp6 - \beta)P_m^n - S(m)\right\} / (\beta + temp1b + temp2b + temp3b + temp4b + temp5b + temp6b) \quad (3.79)$$

Line 3 i=2: (N_x-1), j=N_y, k=1

$$P_m^{n+1} = \{\left(temp1bP_{m+1}^{n+1} + temp2bP_{m-1}^{n+1} + (temp3b + temp4b)P_{m-N_x}^{n+1} + (temp5b + temp6b)P_{m+N_2}^{n+1}\right) + \left(temp1P_{m+1}^{n} + temp2P_{m-1}^{n} + (temp3 + temp4)P_{m-N_x}^{n} + (temp5 + temp6)P_{m+N_2}^{n}\right) - (temp1 + temp2 + temp3 + temp4 + temp5 + temp6 - \beta)P_m^n - S(m)\}/(\beta + temp1b + temp2b + temp3b + temp4b + temp5b + temp6b) \quad (3.80)$$

Line 7 i=N_x, j=N_y, k=2: (N_z-1)

$$P_m^{n+1} = \{\left(\left((temp1b + temp2b)P_{m-1}^{n+1} + (temp3b + temp4b)P_{m-N_x}^{n+1} + temp5bP_{m+N_2}^{n+1} + temp6bP_{m-N_2}^{n+1}\right)\right) + \left((temp1 + temp2)P_{m-1}^{n} + (temp3 + temp4)P_{m-N_x}^{n} + temp5P_{m+N_2}^{n} + temp6P_{m-N_2}^{n}\right) - (temp1 + temp2 + temp3 + temp4 + temp5 + temp6 - \beta)P_m^n - S(m)\}/(\beta + temp1b + temp2b + temp3b + temp4b + temp5b + temp6b) \quad (3.81)$$

Line 11 i=2: (N_x-1), j=N_y, k=N_z

$$P_m^{n+1} = \{\left(temp1bP_{m+1}^{n+1} + temp2bP_{m-1}^{n+1} + (temp3b + temp4b)P_{m-N_x}^{n+1} + (temp5b + temp6b)P_{m-N_2}^{n+1}\right) + \left(temp1P_{m+1}^{n} + temp2P_{m-1}^{n} + (temp3 + temp4)P_{m-N_x}^{n} + (temp5 + temp6)P_{m-N_2}^{n}\right) - (temp1 + temp2 + temp3 + temp4 + temp5 + temp6 - \beta)P_m^n - S(m)\}/(\beta + temp1b + temp2b + temp3b + temp4b + temp5b + temp6b) \quad (3.82)$$

Line 8 i=1, j=N_y, k=2: (N_z-1)

$$P_m^{n+1} = \{\left(\left((temp1b + temp2b)P_{m+1}^{n+1} + (temp3b + temp4b)P_{m-N_x}^{n+1} + temp5bP_{m+N_2}^{n+1} + temp6bP_{m-N_2}^{n+1}\right)\right) + \left((temp1 + temp2)P_{m+1}^{n} + (temp3 + temp4)P_{m-N_x}^{n} + temp5P_{m+N_2}^{n} + temp6P_{m-N_2}^{n}\right) - (temp1 + temp2 + temp3 + temp4 + temp5 + temp6 - \beta)P_m^n - S(m)\}/(\beta + temp1b + temp2b + temp3b + temp4b + temp5b + temp6b) \quad (3.83)$$

3.4.3.4 For the faces

Face 1 i=1, j=2: (N_y-1), k=2: (N_z-1)

$$P_m^{n+1} = \left\{\left((temp1b + temp2b)P_{m+1}^{n+1} + temp3bP_{m+N_x}^{n+1} + temp4bP_{m-N_x}^{n+1} + temp5bP_{m+N_2}^{n+1} + temp6bP_{m-N_2}^{n+1}\right) + \left((temp1 + temp2)P_{m+1}^{n} + temp3P_{m+N_x}^{n} + temp4P_{m-N_x}^{n} + temp5P_{m+N_2}^{n} + temp6P_{m-N_2}^{n}\right) - (temp1 + temp2 + temp3 + temp4 + temp5 + temp6 - \beta)P_m^n - S(m)\right\}/(\beta + temp1b + temp2b + temp3b + temp4b + temp5b + temp6b) \quad (3.84)$$

Face 2 i=N_x, j=2: (N_y-1), k=2: (N_z-1)

$$P_m^{n+1} = \left\{\left((temp1b + temp2b)P_{m+1}^{n+1} + temp3bP_{m+N_x}^{n+1} + temp4bP_{m-N_x}^{n+1} + temp5bP_{m+N_2}^{n+1} + temp6bP_{m-N_2}^{n+1}\right) + \left((temp1 + temp2)P_{m+1}^{n} + temp3P_{m+N_x}^{n} + temp4P_{m-N_x}^{n} + temp5P_{m+N_2}^{n} + temp6P_{m-N_2}^{n}\right) - (temp1 + temp2 + temp3 + temp4 + temp5 + temp6 - \beta)P_m^n - S(m)\right\}/(\beta + temp1b + temp2b + temp3b + temp4b + temp5b + temp6b) \quad (3.85)$$

Face 5 i= 2: (N_x-1), j=1, k=2: (N_z-1)

$$P_m^{n+1} = \left\{\left(temp1bP_{m+1}^{n+1} + temp2bP_{m-1}^{n+1} + (temp3b + temp4b)P_{m+N_x}^{n+1} + temp5bP_{m+N_2}^{n+1} + temp6bP_{m-N_2}^{n+1}\right) + \left(temp1P_{m+1}^{n} + temp2P_{m-1}^{n} + (temp3b + temp4b)P_{m+N_x}^{n+1} + temp5P_{m+N_2}^{n} + temp6P_{m-N_2}^{n}\right) - (temp1 + temp2 + temp3 + temp4 + temp5 + temp6 - \beta)P_m^n - S(m)\right\}/(\beta + temp1b + temp2b + temp3b + temp4b + temp5b + temp6b) \quad (3.86)$$

Face 6 i=2: (N_x-1), j=N_y, k=2: (N_z-1)

$$P_m^{n+1} = \left\{\left(temp1bP_{m+1}^{n+1} + temp2bP_{m-1}^{n+1} + (temp3b + temp4b)P_{m-N_x}^{n+1} + temp5bP_{m+N_2}^{n+1} + temp6bP_{m-N_2}^{n+1}\right) + \left(temp1P_{m+1}^{n} + temp2P_{m-1}^{n} + (temp3b + temp4b)P_{m-N_x}^{n+1} + temp5P_{m+N_2}^{n} + temp6P_{m-N_2}^{n}\right) - (temp1 + temp2 + temp3 + temp4 + temp5 + temp6 - \beta)P_m^n - S(m)\right\}/(\beta + temp1b + temp2b + temp3b + temp4b + temp5b + temp6b) \quad (3.87)$$

Face 3 i=2: (Nx-1), j=2: (Ny-1), k=1

$$P_m^{n+1} = \{(temp1bP_{m+1}^{n+1} + temp2bP_{m-1}^{n+1} + temp3bP_{m+N_x}^{n+1} + temp4bP_{m-N_x}^{n+1} + (temp5b + temp6b)P_{m+N_2}^{n+1}) + (temp1P_{m+1}^{n} + temp2P_{m-1}^{n} + temp3P_{m+N_x}^{n} + temp4P_{m-N_x}^{n} + (temp5b + temp6b)P_{m+N_2}^{n+1}) - (temp1 + temp2 + temp3 + temp4 + temp5 + temp6 - \beta)P_m^n - S(m)\}/(\beta + temp1b + temp2b + temp3b + temp4b + temp5b + temp6b) \quad (3.88)$$

Face 4 i=2: (Nx-1), j=2: (Ny-1), k=Nz

$$P_m^{n+1} = \{(temp1bP_{m+1}^{n+1} + temp2bP_{m-1}^{n+1} + temp3bP_{m+N_x}^{n+1} + temp4bP_{m-N_x}^{n+1} + (temp5b + temp6b)P_{m-N_2}^{n+1}) + (temp1P_{m+1}^{n} + temp2P_{m-1}^{n} + temp3P_{m+N_x}^{n} + temp4P_{m-N_x}^{n} + (temp5b + temp6b)P_{m\pm}^{n+1}) - (temp1 + temp2 + temp3 + temp4 + temp5 + temp6 - \beta)P_m^n - S(m)\}/(\beta + temp1b + temp2b + temp3b + temp4b + temp5b + temp6b) \quad (3.89)$$

The MATLAB programming underwent these summarized under listed steps:

- Temperature model in which reservoir description such as overall geometry, grid size specification and its thermal properties; thermal conductivity, specific heat capacity and density were outlined. The location and amount of heat source were specified.
- Viscosity model for which initial reservoir viscosity has been stated
- Pressure model which has its rock and fluid properties (permeability, porosity, formation volume factor and viscosity) being outlined. The location of the horizontal well is specified with the rate at which it is producing.
- The execution of the program starts with the computation of the new temperatures which has been coupled with the viscosity model to give new viscosities in the system which in turn helps in the computation of the new pressures. Following these is the computation of average reservoir pressure.

- The visual output display of the sequence which include 3D surface plots of temperature, viscosity and pressure all after each time step. Also there are plots of viscosity, temperature and pressure over time. Figure 3.4 shows the outlined steps.

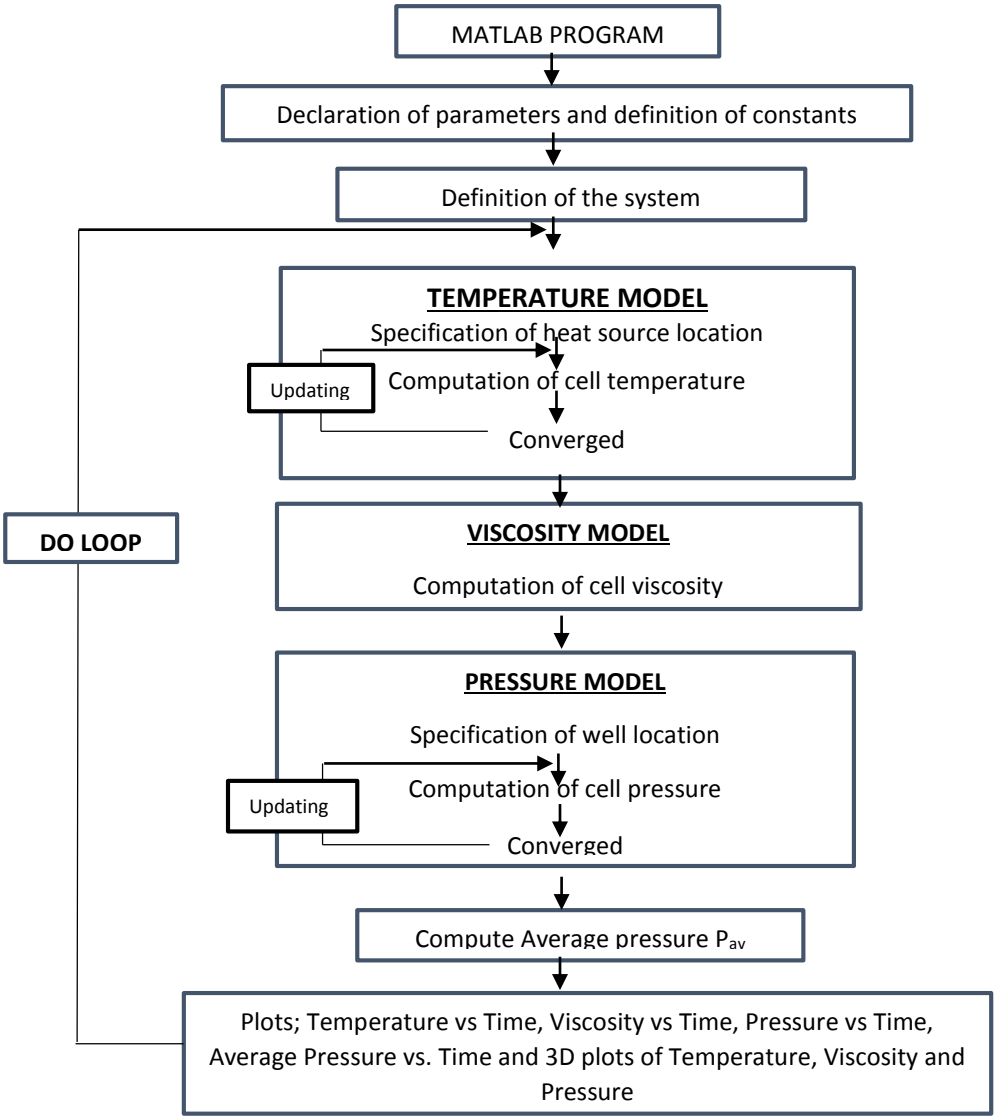

Figure 3.4: MATLAB sequential process algorithm

Average reservoir pressure P_{av} is computed using;

$$P_{av} = \frac{\sum_{i=1,j=1,k=1}^{n} Pn(m) * N_p(m)}{N_{ps}}$$

Where

The cumulative production, N_p from each cell is computed using the formula;

$$N_p(m) = \frac{\Delta V * \emptyset * (1 - S_w) * C_e * \Delta P(m)}{B_o(m)}$$

The cumulative production of entire reservoir N_{ps} is computed using;

$$N_{ps} = \sum_{i=1,j=1,k=1}^{n} N_p(m)$$

The oil formation volume factor, B_o for each cell is computed using the relation;

$$B_o(m) = B_{ob}[1 - C_o(P(m) - P_{ob})]$$

$$\Delta P(m) = P_m^n - P_m^{n+1}$$

CHAPTER FOUR

RESULTS AND DISCUSSION

This chapter focuses on the plots of temperature, viscosity and pressure both in 2D and 3D and their analysis. This model was run using a grid size of 11*11*11 since the computer storage was too small to run a higher grid size.

4.1 Base Case Scenario

The model is run firstly without any heat source to observe the bottom-hole and average pressure in the reservoir that is, no change in temperature and viscosity. Figure 4.1 shows that the average reservoir pressure (Pav) is higher than the bottom-hole flowing pressure (Pwf) thus there being production. It can also be observed that both pressures decline with time. It is expected that for a volumetric reservoir, the pressure decline would be rapid over time.

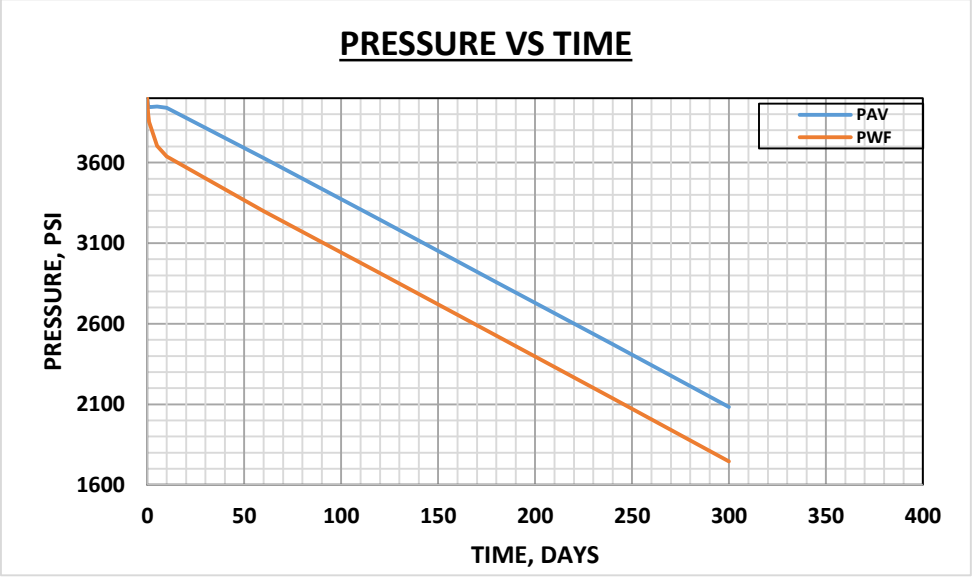

Figure 4.1: A plot of Pressure (Pav, Pwf) versus Time.

4.2 Thermal Process

The model is then run with a heat source of 250 W/m^3. Plots from temperature, viscosity and pressure are all analyzed. Figure 4.2.1 shows an initial decrease of the line followed by a rise in the line with normalized line till the end. The plot is for the cell at the center of the reservoir where both the heat source and the well are located. This initial decrease is due to some of the heat produced being lost to the fluid that is being produced through the wellbore while a significant amount of that same heat is being radiated out to neighboring cells. Different slopes are observed from the graph which can also be attributed to some amount of heat being lost to the fluid produced through wellbore while the cooler fluids coming from the neighboring cells mixes with the fluid left at the center cell till equilibrium is reached between the two fluids. The temperature rise would be minimal till the radiated heat reaches the point of equilibrium with the neighboring cells after which the temperature at the wellbore increase.

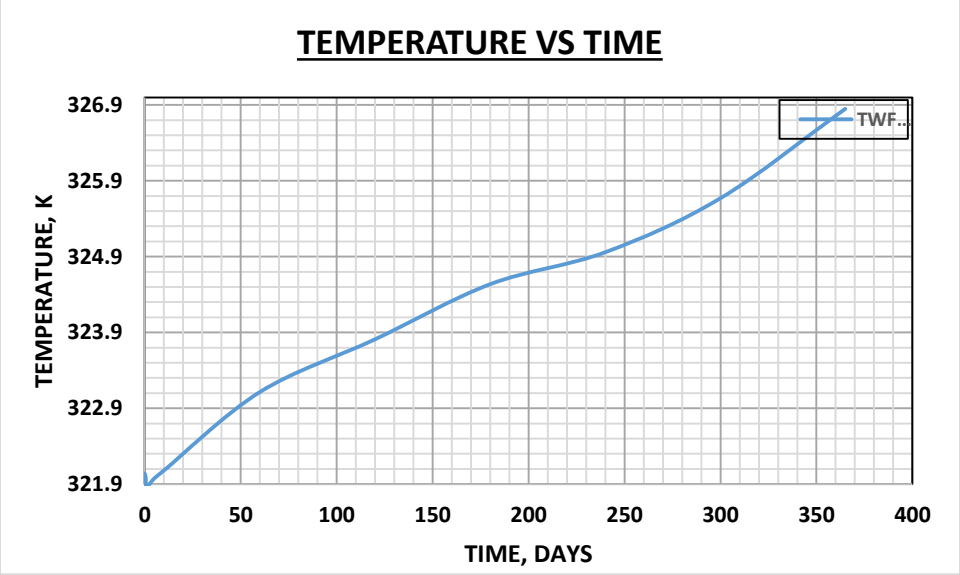

Figure 4.2.1: A plot of Temperature (Twf)) versus Time.

Figure 2.1.2 shows the behavior of temperature over time for some selected cells; a cell at the boundary (TAB), in between the boundary and the center (Tin) and just around the center (Tjac). It can be seen that their behavior are different. Both Tin and TAB shows almost linear behavior which is due to the heat being radiated out to them and no significant heat loss achieved. For Tjac, it receives enough heat at the initial stage which is not lost to withdrawal but only to radiating out the neighboring cells but a point in time the impact of withdrawal is felt which shows the sudden decrease in temperature.

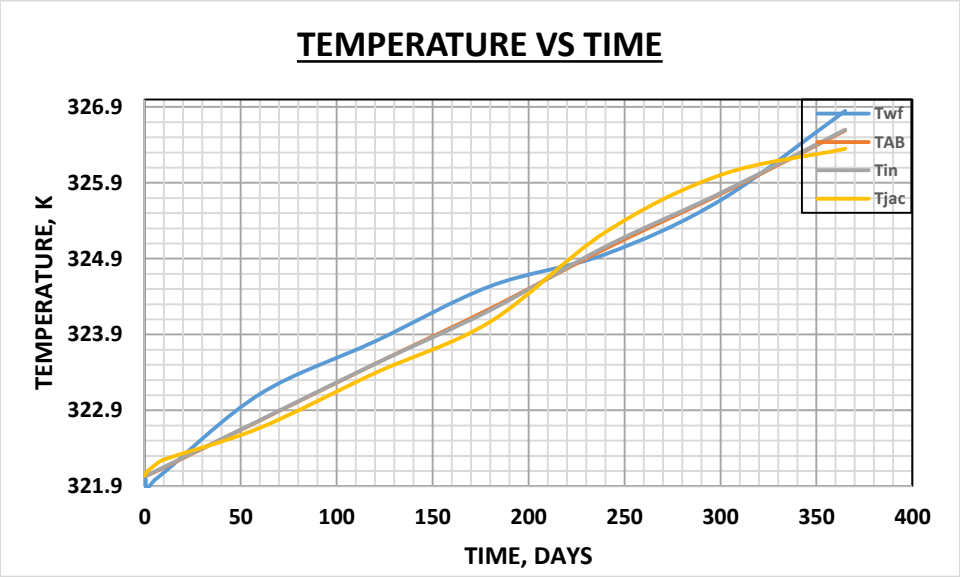

Figure 4.2.2: A plot of Temperature (Twf, TAB, Tin, Tjac) versus Time.

Figure 4.2.3 – 10 shows the surface temperature distribution after several days. At the center, for the first 10 days, the heat being emitted from the probe was lost to both the fluid produced through wellbore and the surrounding cells due to radiating out. After 60 days till 365 days, the temperature increase was gradual process which can also be attributed to heat loss through the wellbore, heat radiating out to the other cells and also cooler fluids moving into the center thus a slow increase

in the temperature. The outer cells receive heat at a pace based on the thermal conductivity of the system.

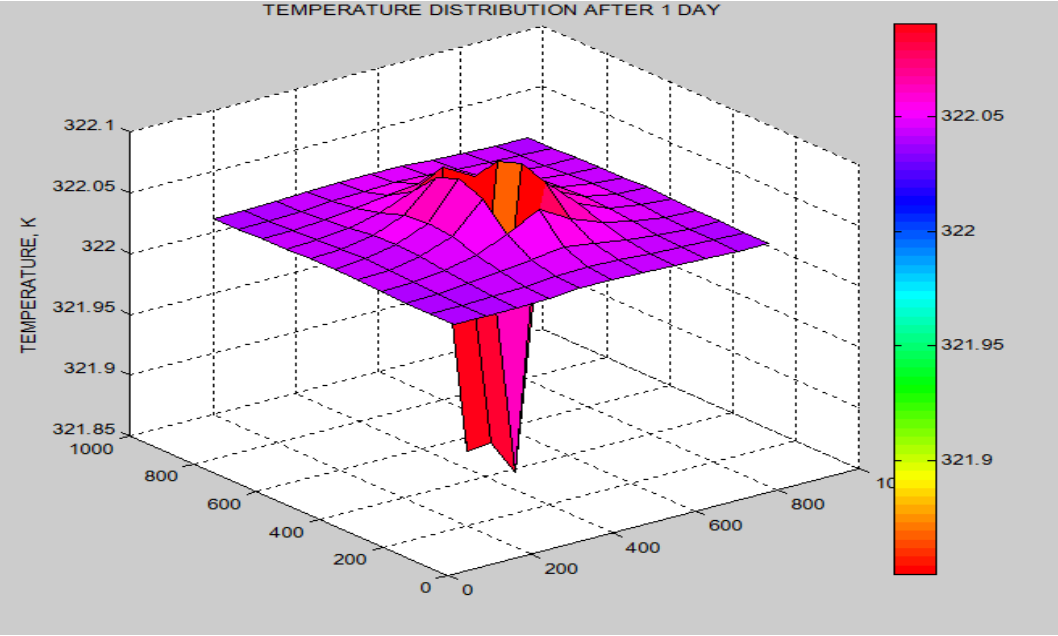

Figure 4.2.3: Surface plot of reservoir temperature distribution after 1 day.

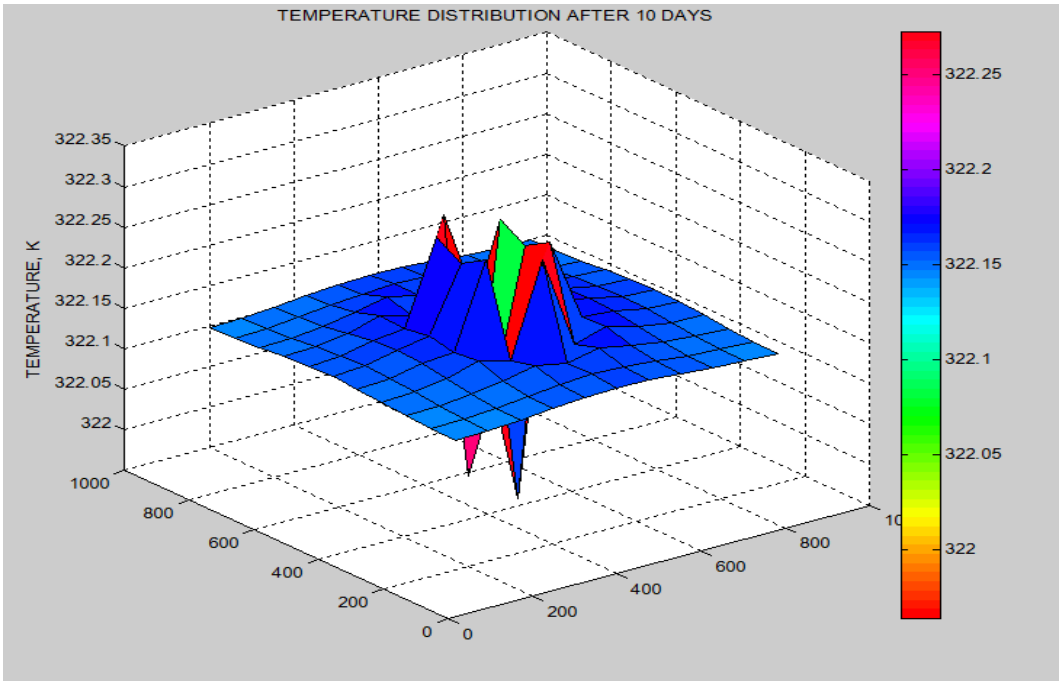

Figure 4.2.4: Surface plot of reservoir temperature distribution after 10 days.

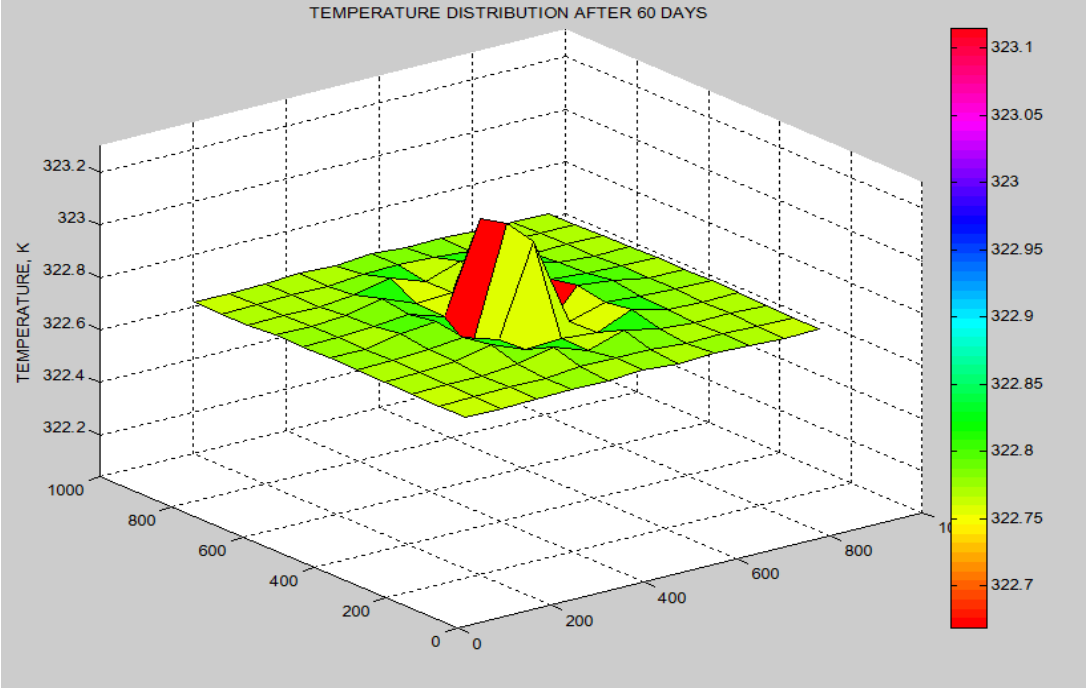

Figure 4.2.5: Surface plot of reservoir temperature distribution after 60 days.

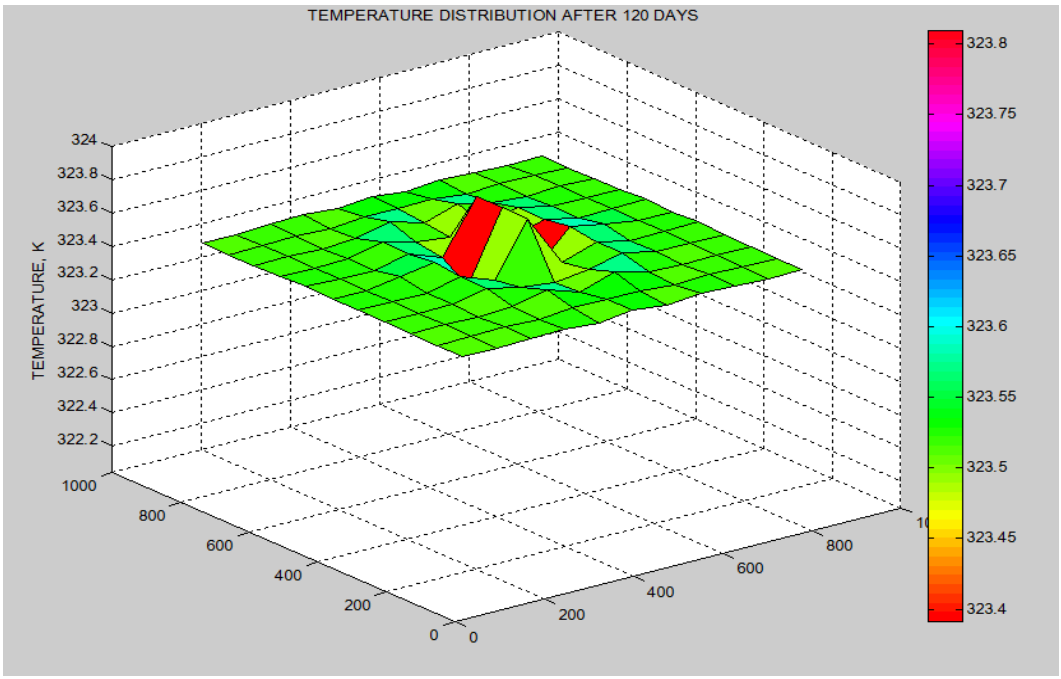

Figure 4.2.6: Surface plot of reservoir temperature distribution after 120 days.

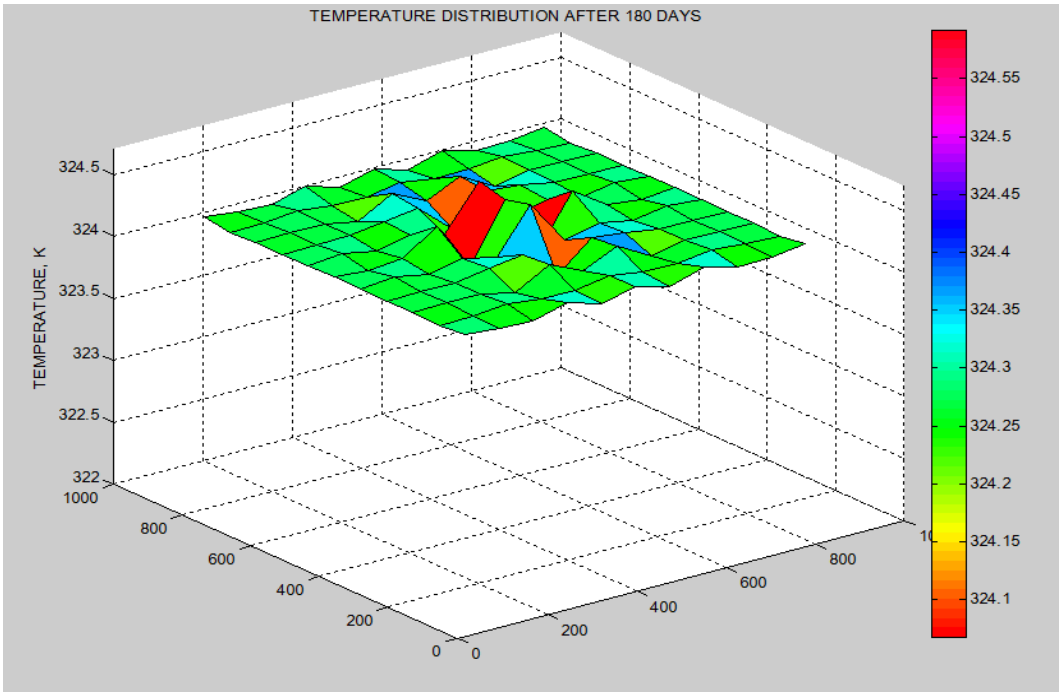

Figure 4.2.7: Surface plot of reservoir temperature distribution after 180 days.

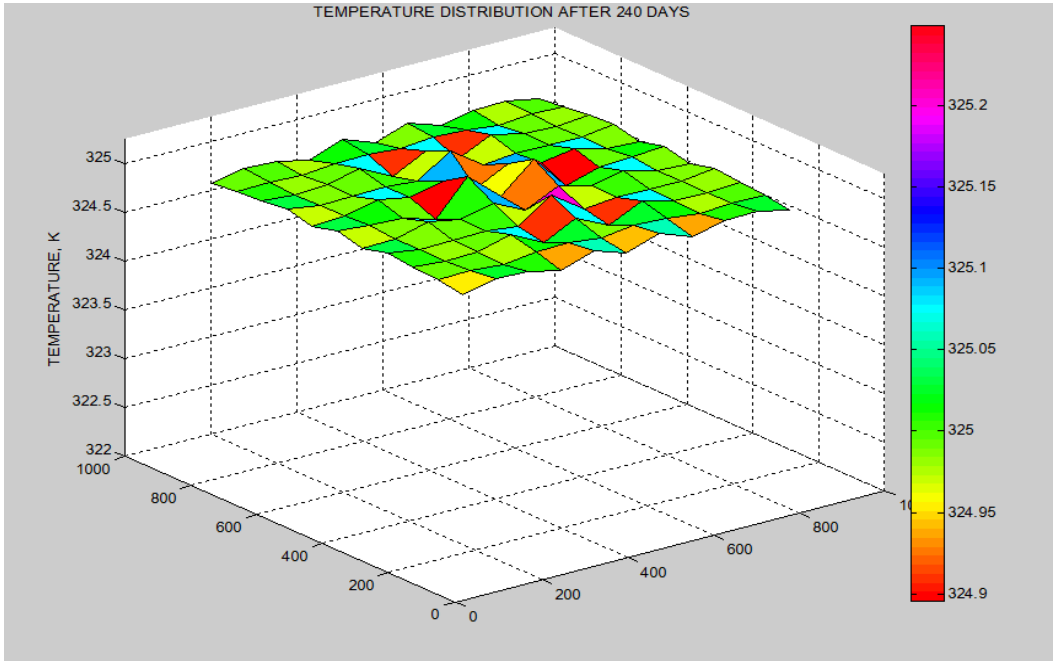

Figure 4.2.8: Surface plot of reservoir temperature distribution after 240 days.

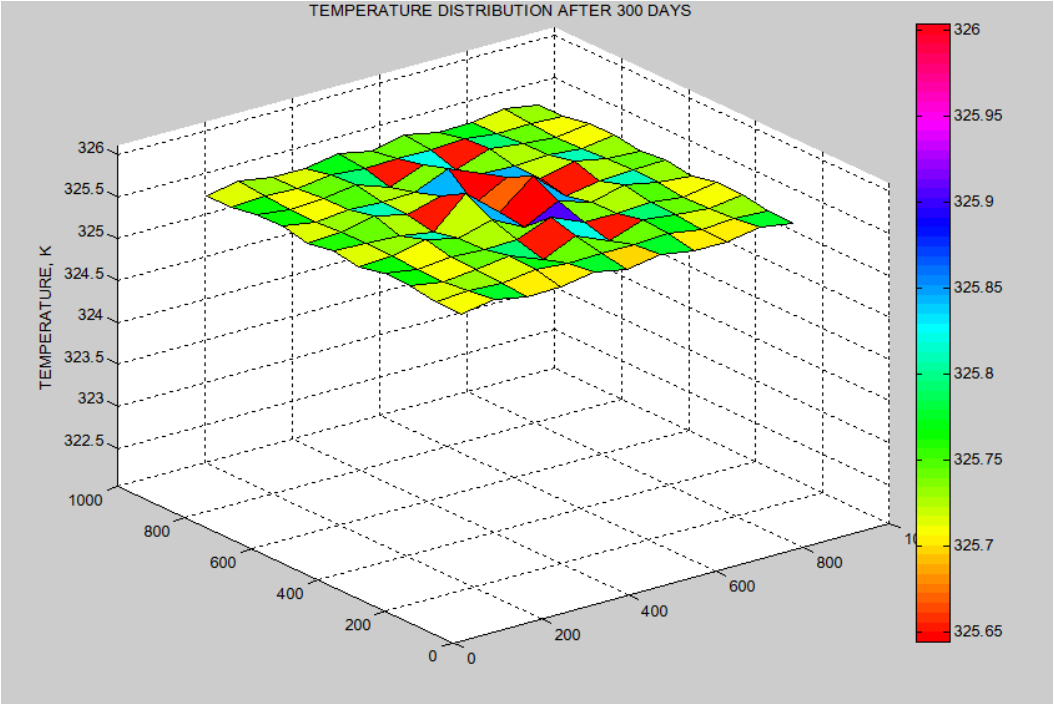

Figure 4.2.9: Surface plot of reservoir temperature distribution after 300 days.

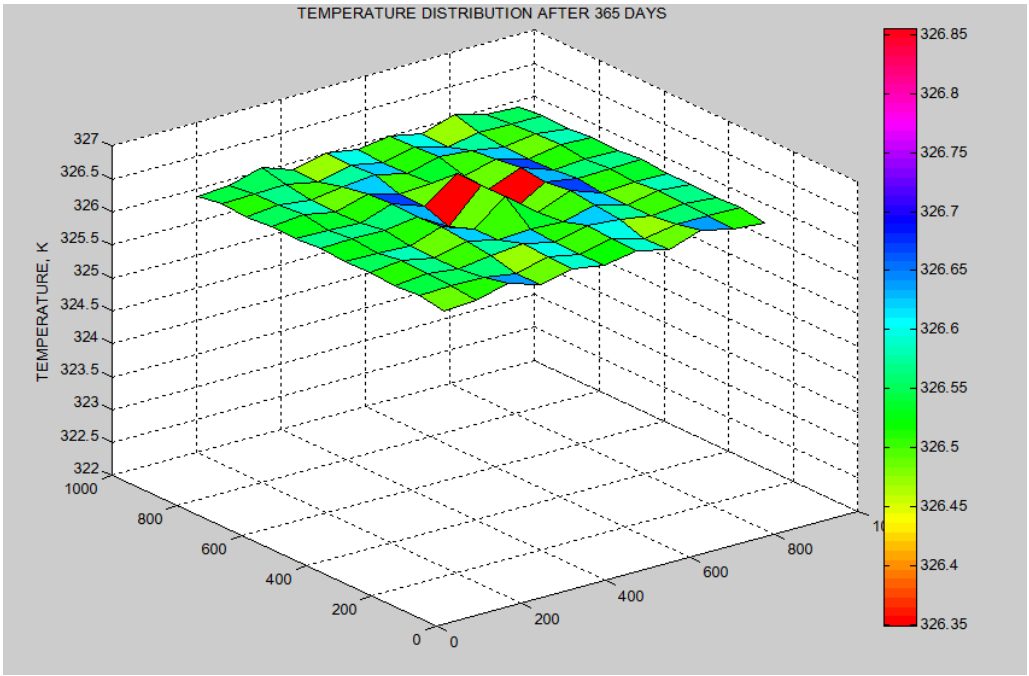

Figure 4.2.10: Surface plot of reservoir temperature distribution after 365 days.

Figure 4.2.11 depicts the behavior of the viscosity for the center cell (Vwf) based on its temperature behavior. An increase in temperature tend to increase the molecular energy thus decrease the intermolecular force between the molecules of the fluid and making the movement of the molecules free. A gradual increase in temperature result in a gradual decrease in the viscosity and vice versa.

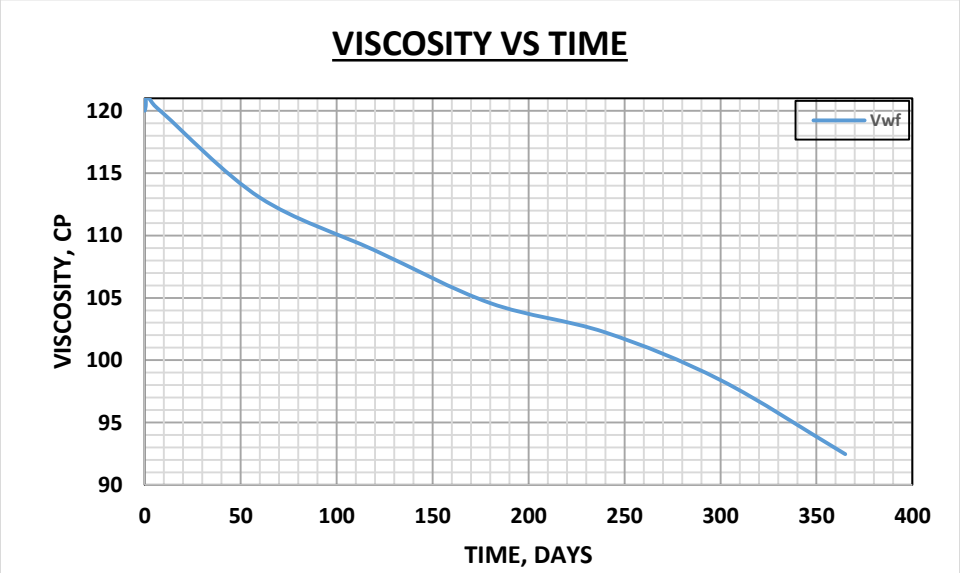

Figure 4.2.11: A plot of Viscosity (Vwf) versus Time.

Figure 4.2.12 shows the behavior of the same selected cells (VAB, Vjac, Vin) for the temperature plot based on the temperature behavior. An increase in temperature affect the viscosity by reducing it.

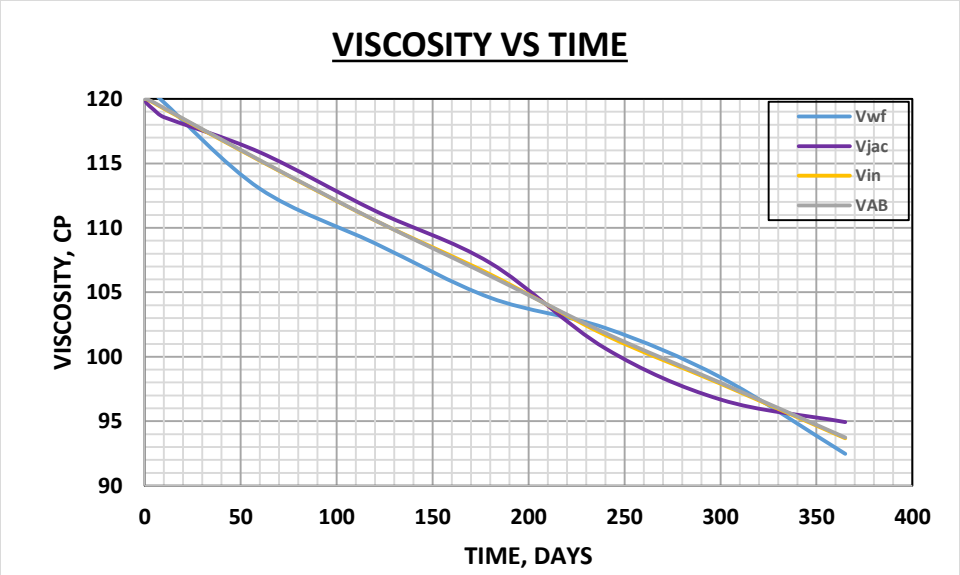

Figure 4.2.12: A plot of Viscosity (Vwf, Vjac, Vin, VAB) versus Time.

From figure 4.2.13 – 20, the behavior of the different cell viscosities are seen after 365 days. These viscosities are as result of their temperature behavior; the higher the temperature, the lower the viscosity and vice versa.

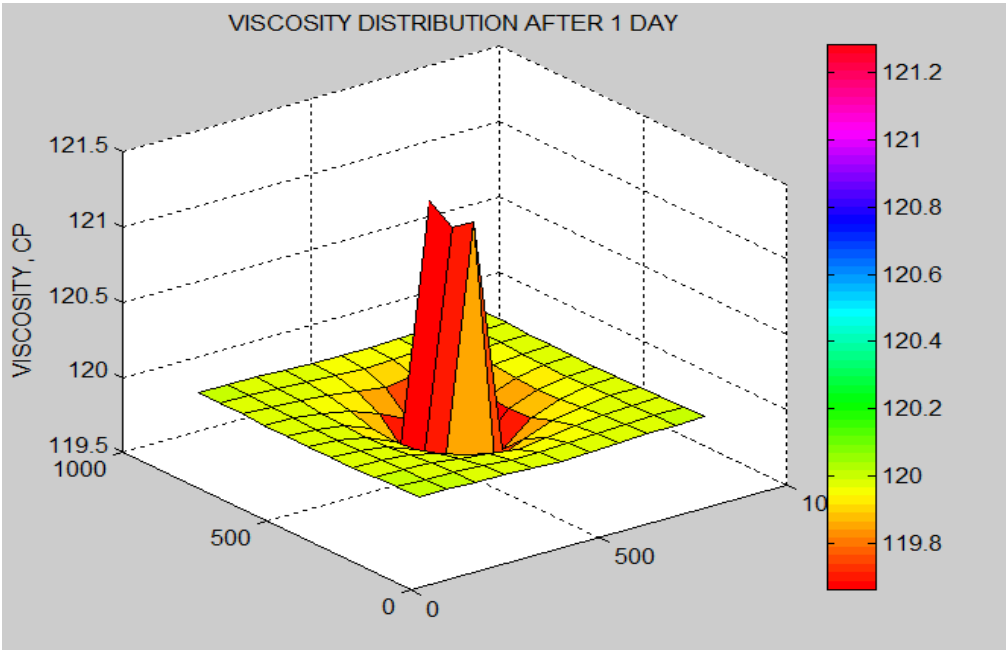

Figure 4.2.13: Surface plot of viscosity distribution after 1 day.

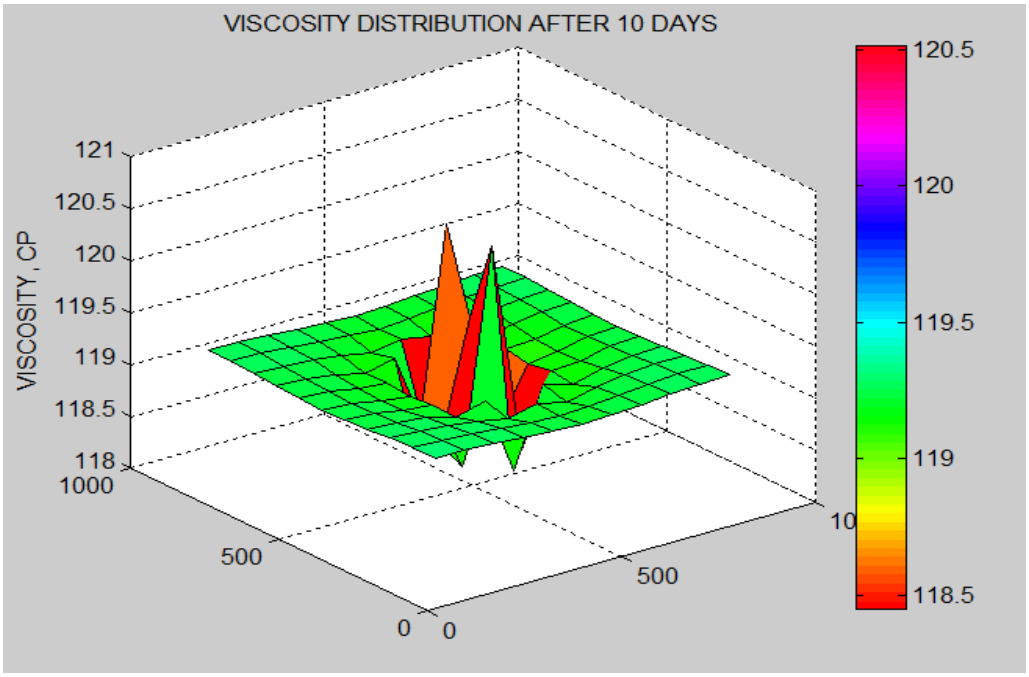

Figure 4.2.14: Surface plot of viscosity distribution after 10 days.

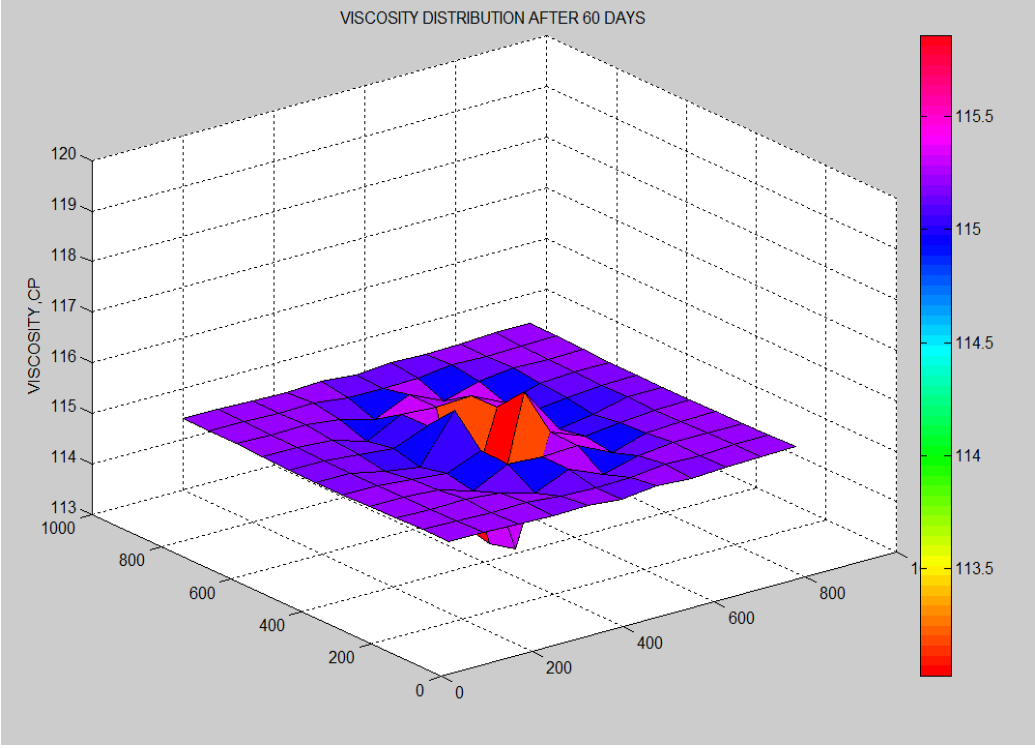

Figure 4.2.15: Surface plot of viscosity distribution after 60 days.

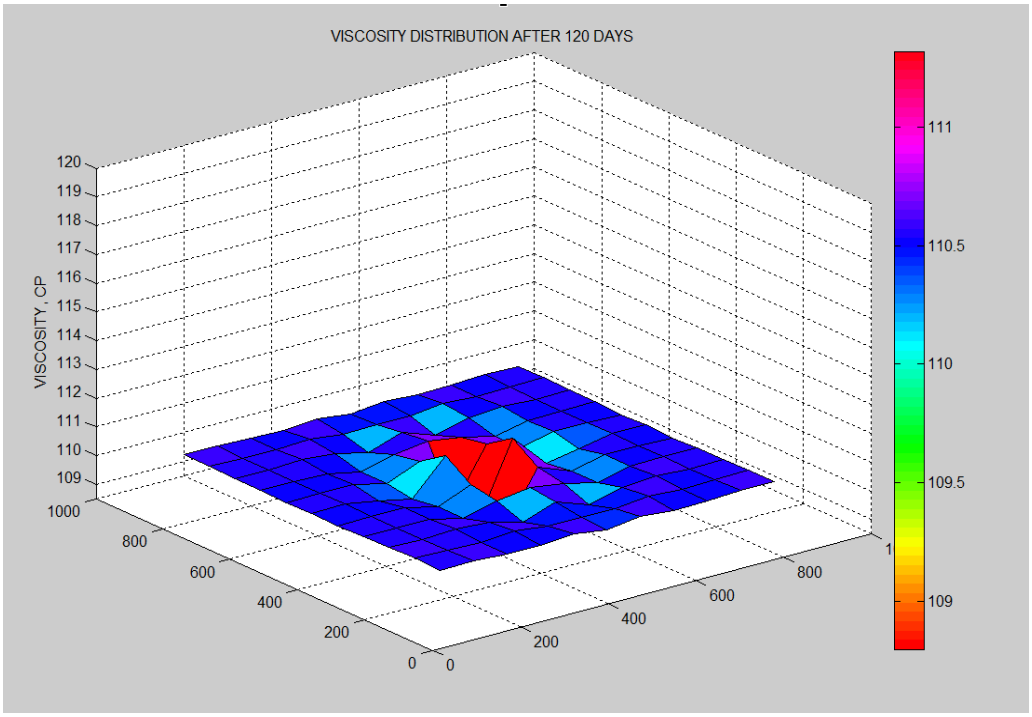

Figure 4.2.16: Surface plot of viscosity distribution after 120 days.

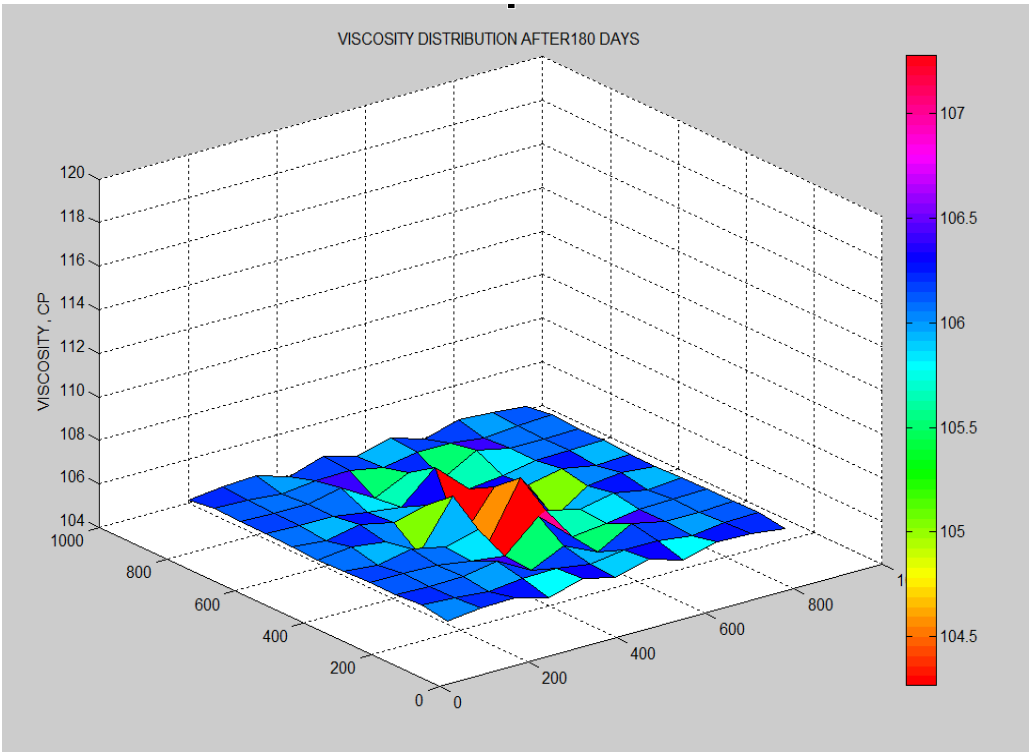

Figure 4.2.17: Surface plot of viscosity distribution after 180 days.

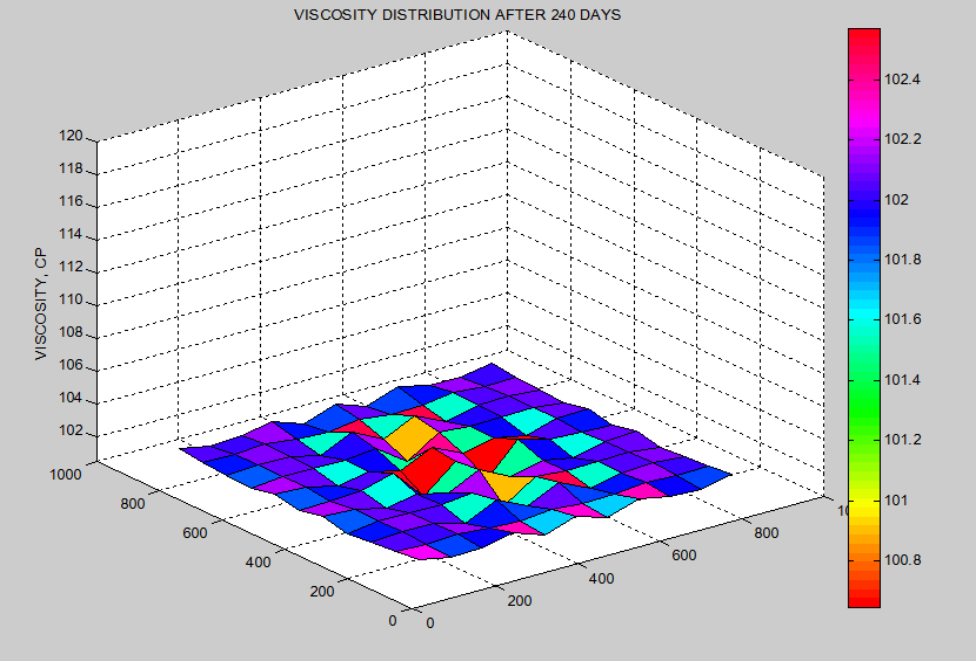

Figure 4.2.18: Surface plot of viscosity distribution after 240 days.

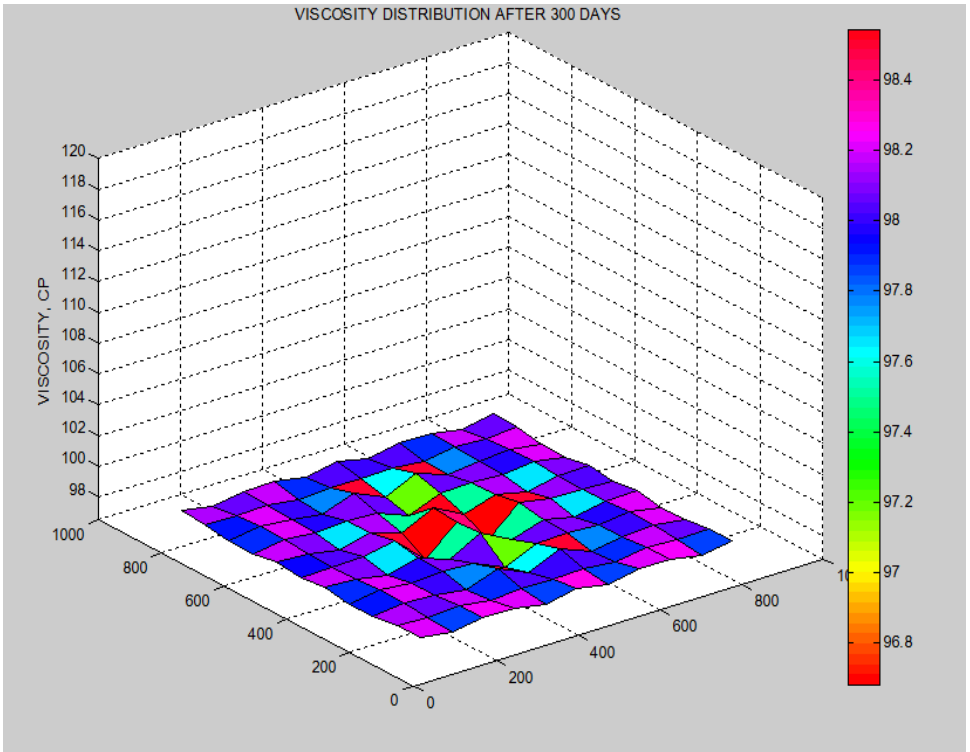

Figure 4.2.19: Surface plot of viscosity distribution after 300 days.

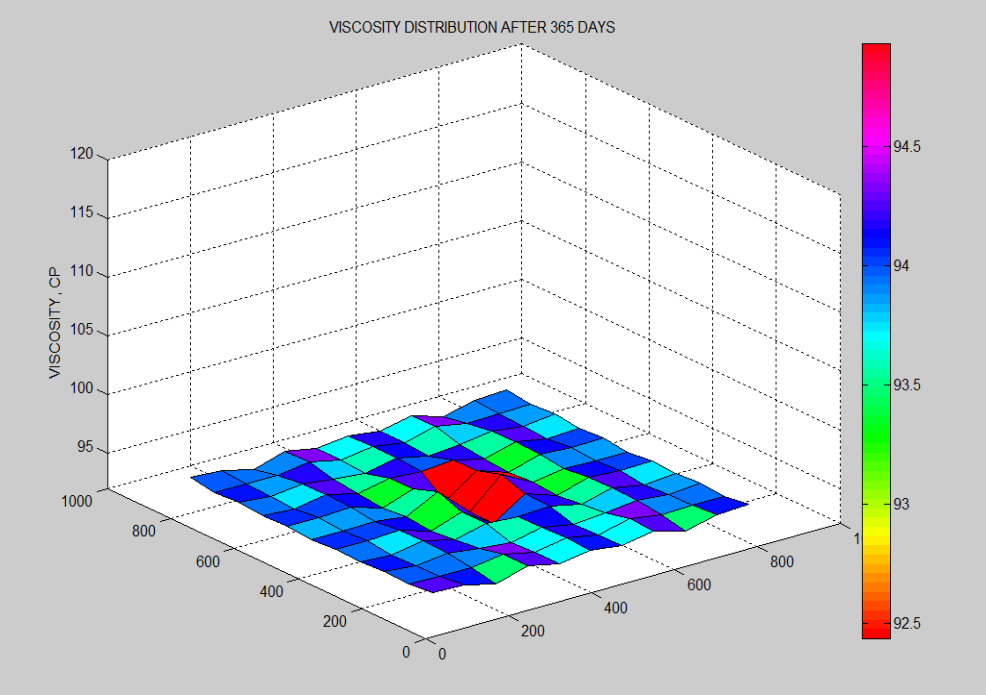

Figure 4.2.20: Surface plot of viscosity distribution after 365 days.

For there to be production there has to be pressure decline. From figure 4.2.21, it can be seen that both bottom hole flowing pressure (Pwf) and average reservoir pressure (Pav) show a sudden decrease in pressure after which the pressure decline is gradual. This can be attributed to the varying viscosity drag in the cell due to the increase in temperature. In comparison with the base case, Figure 4.2.22 shows that the Pwf for the thermal process is higher than the normal volumetric system thus pressure being sustained due to the heating process which reduces the viscosity drag effect. Figure 4.2.23 combines the data of the selected cells from the system while showing their behavior which is dependent on the viscosities thus the temperature variation.

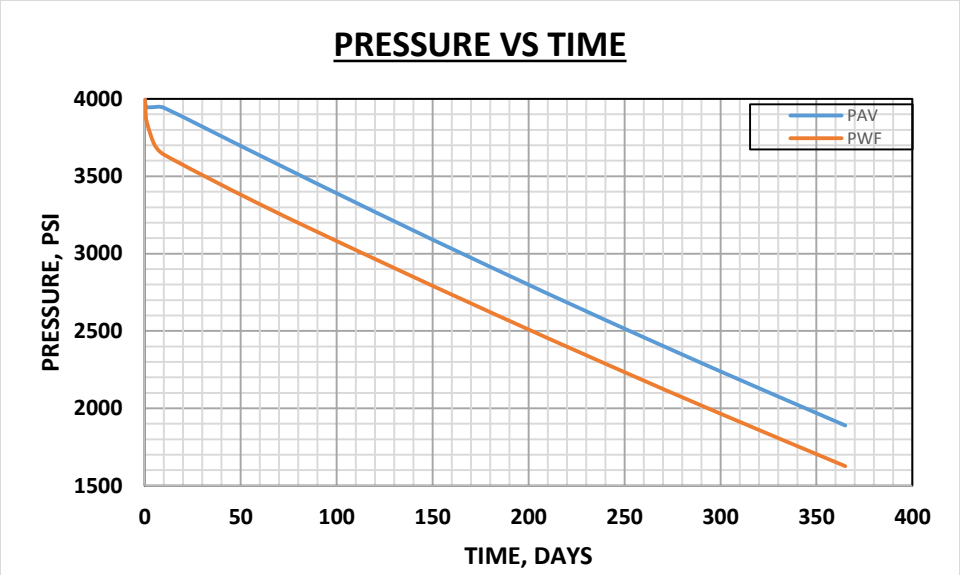

Figure 4.2.21: A plot of Pressure (Pwf, Pav) versus Time.

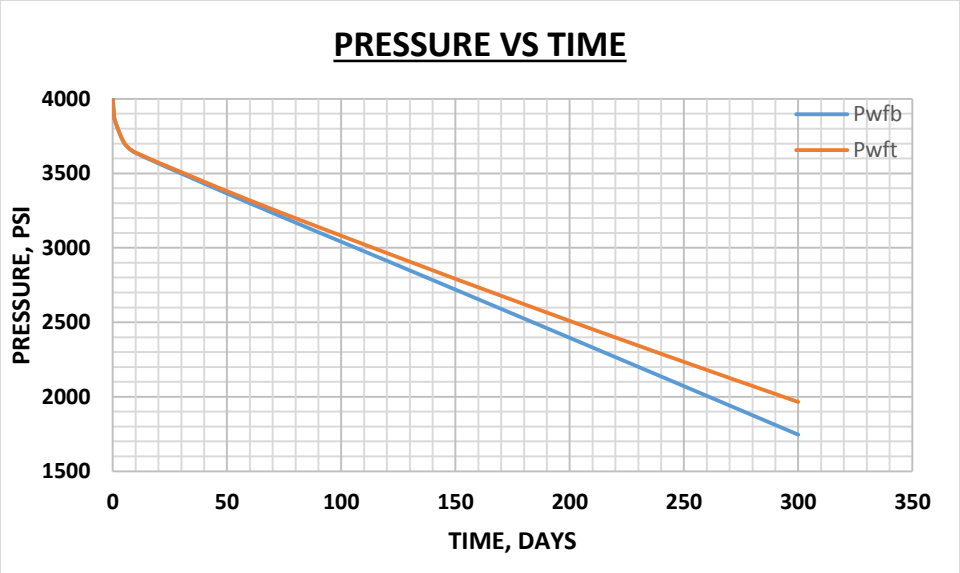

Figure 4.2.22: A plot of Pressure (Pwfb, Pwft) versus Time.

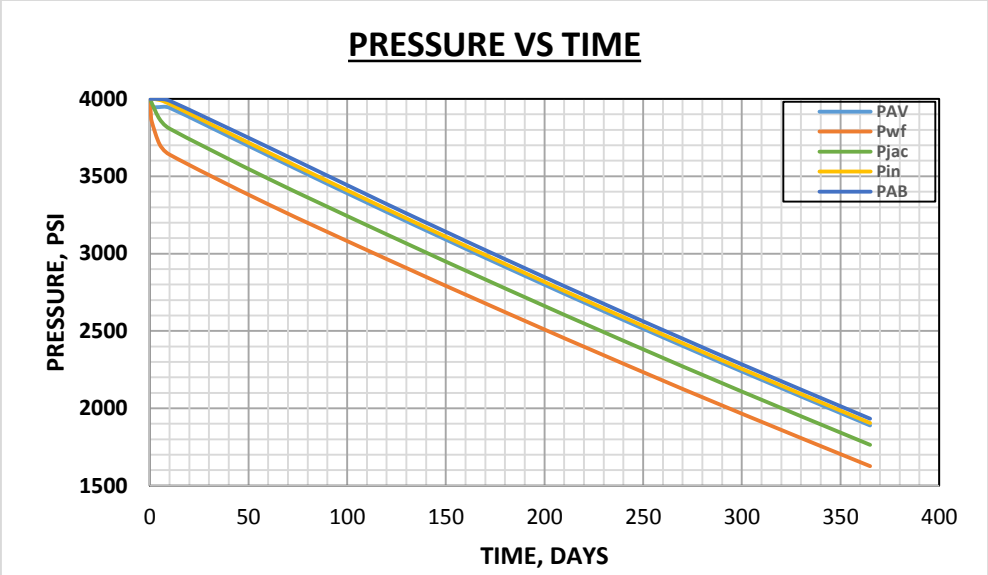

Figure 4.2.23: A plot of Pressure (Pwf, Pin, PAB, Pav, Pjac) versus Time.

From figure 4.2.24 – 31, the behavior of the pressure shows a decline but not a rapid decline such that the decline is slow even with withdrawal being done thus prolonged production life of the reservoir.

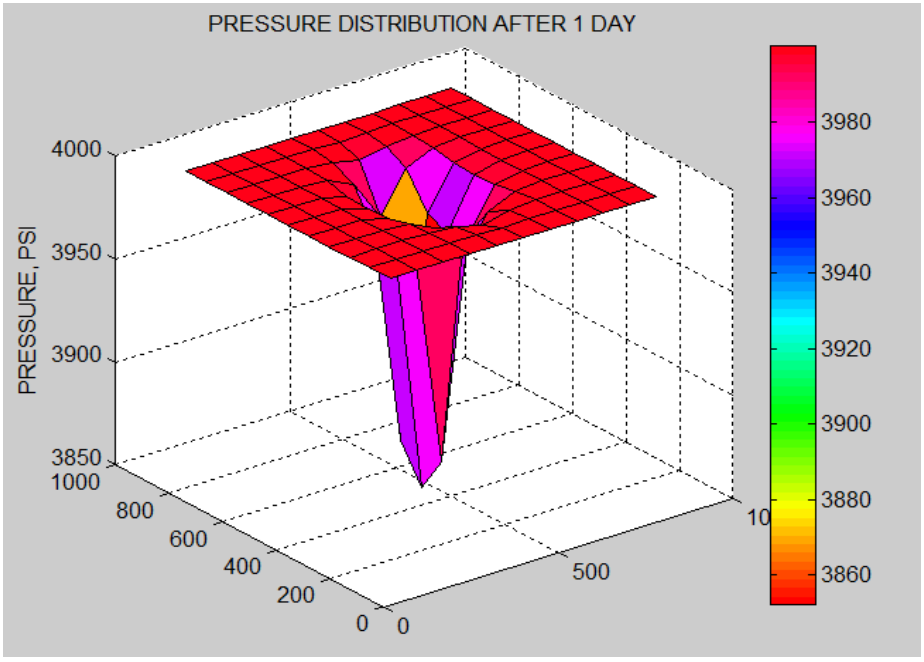

Figure 4.2.24: Surface plot of pressure distribution after 1 day.

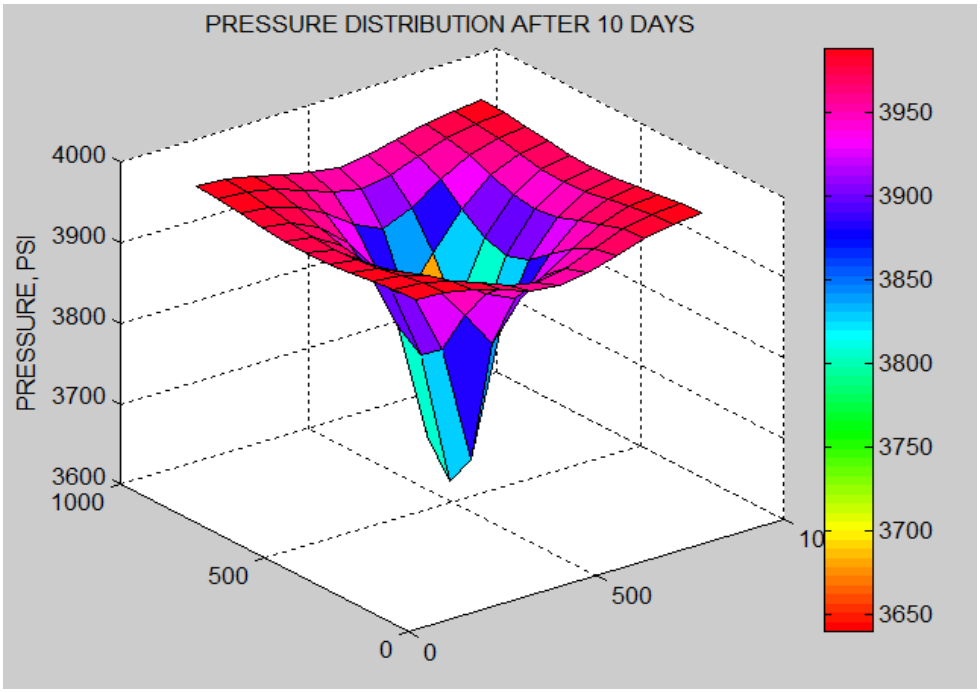

Figure 4.2.25: Surface plot of pressure distribution after 10 days.

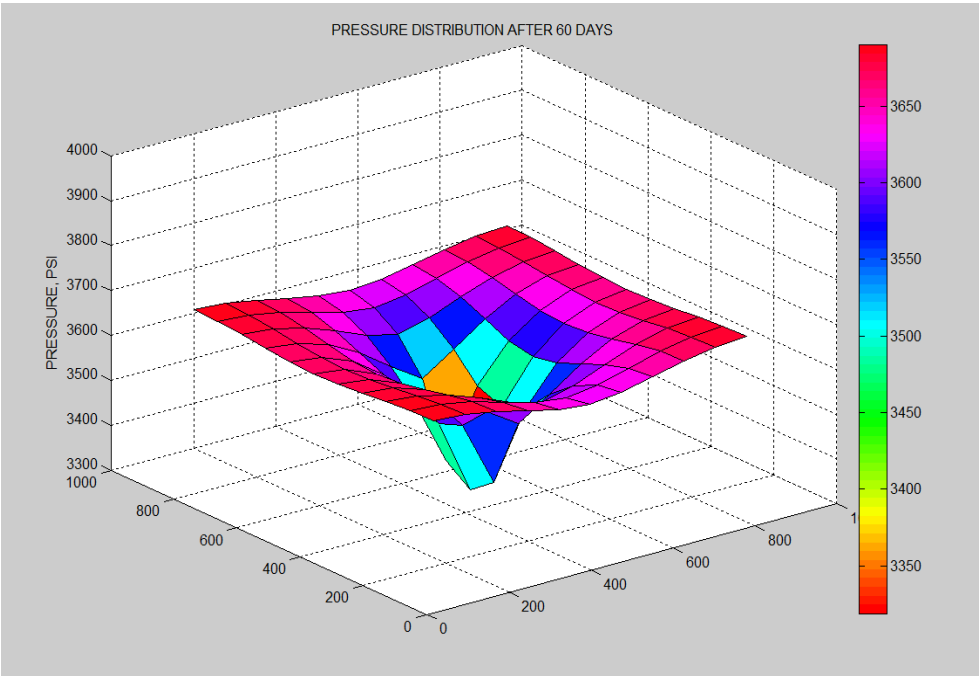

Figure 4.2.26: Surface plot of pressure distribution after 60 days.

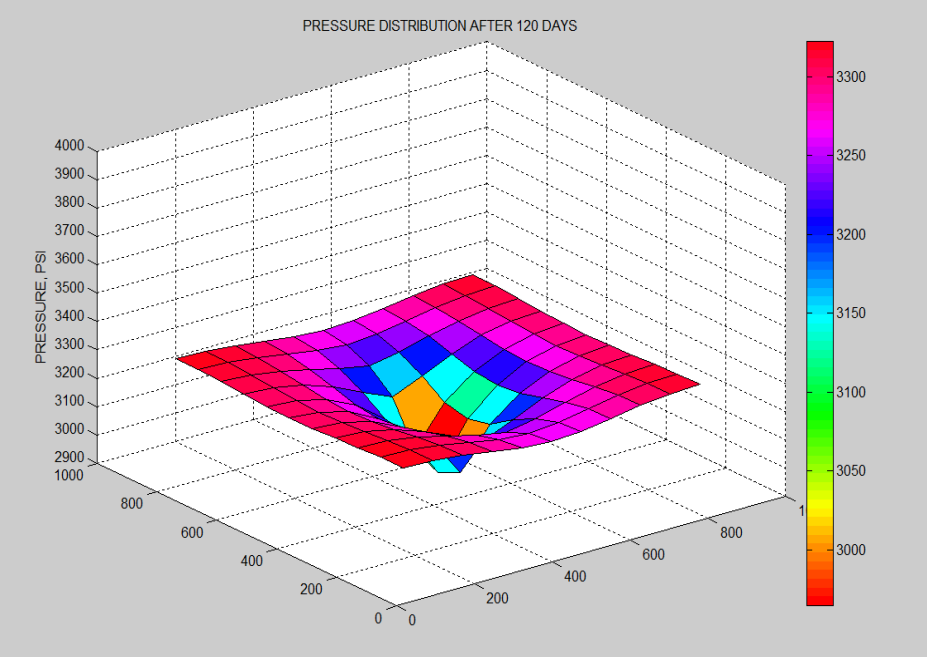

Figure 4.2.27: Surface plot of pressure distribution after 120 days.

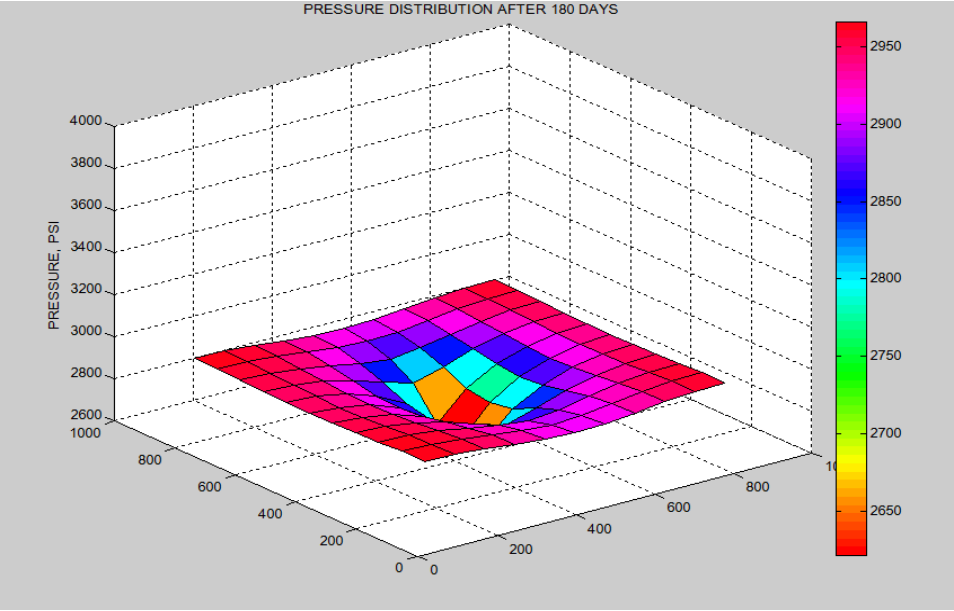

Figure 4.2.28: Surface plot of pressure distribution after 180 days.

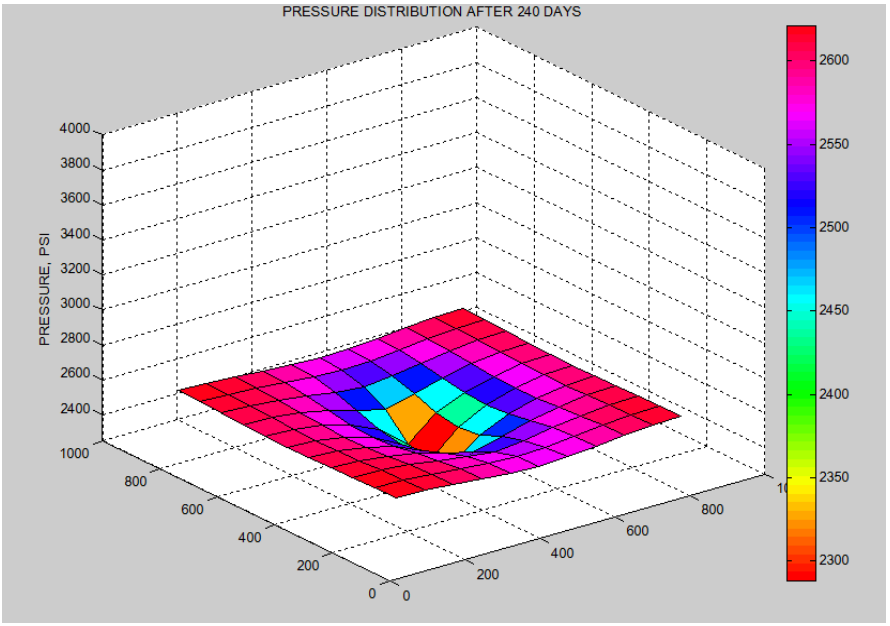

Figure 4.2.29: Surface plot of pressure distribution after 240 days.

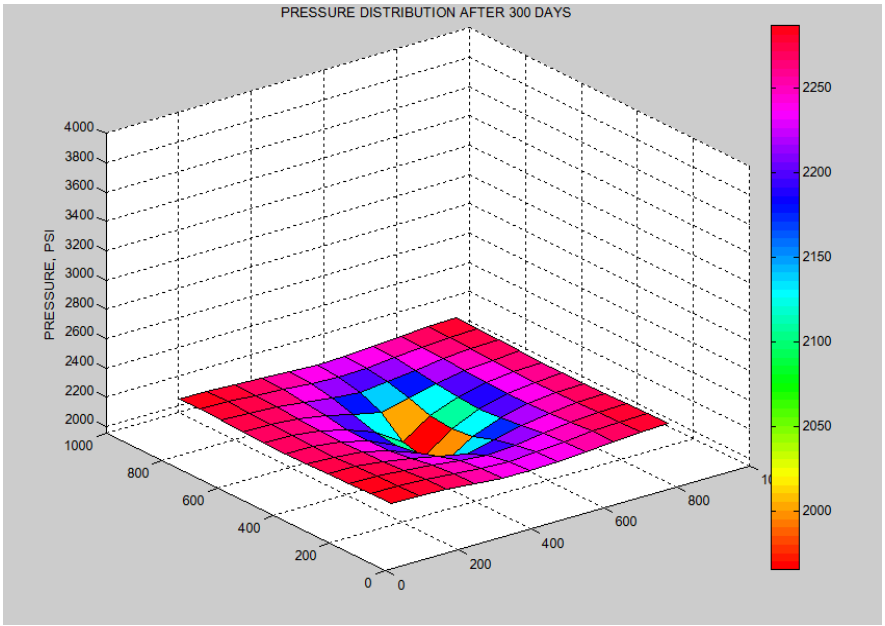

Figure 4.2.30: Surface plot of pressure distribution after 300 days.

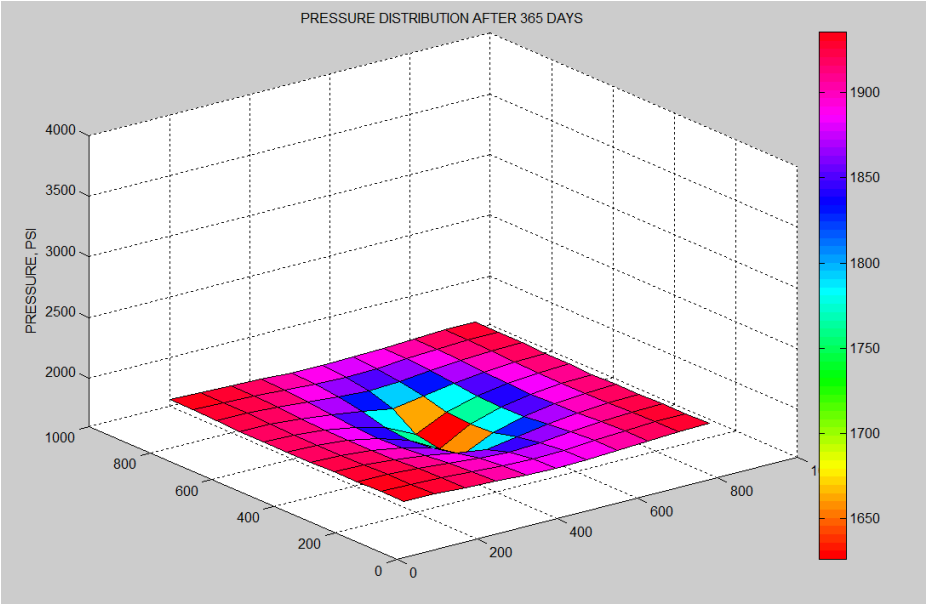

Figure 4.2.31: Surface plot of pressure distribution after 365 days.

4.3 Sensitivity Analysis

The impact of certain key performance parameters such as the heat source introduced is investigated using the developed model. Heat sources of 1000 W/m^3, 500 W/m^3 and 250 W/m^3 were used in the developed model keeping all other parameters constant. Figure 4.3.1 displays the effect of these different heat sources on temperature. It can be seen that with a higher heat source, the heat loss whether to the wellbore or other neighboring cells is not significant and such the temperature rise is almost linear. As the heat source is reduced, the heat loss becomes evident thus the behavior being a slower increase in temperature. The higher the heat source the more rapid the increase in temperature.

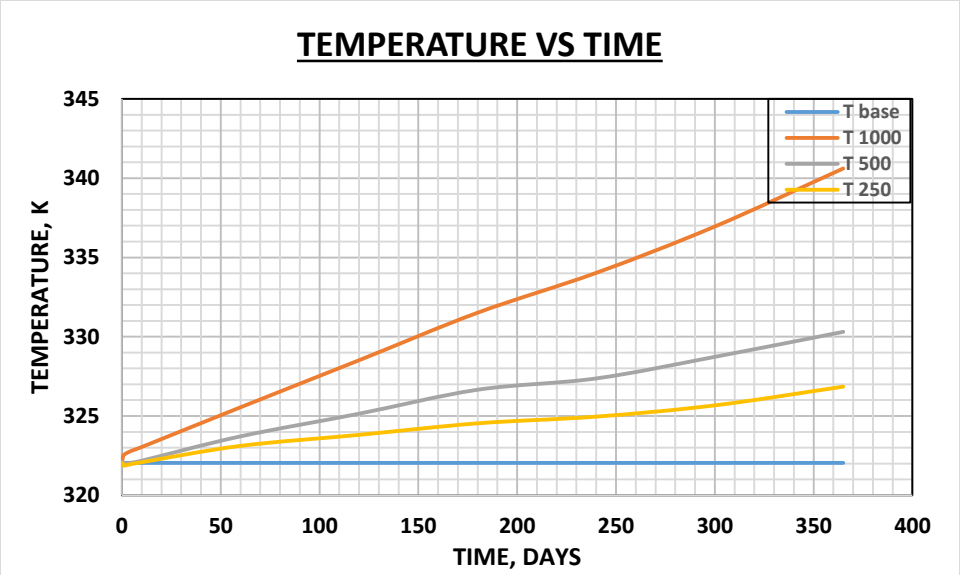

Figure 4.3.1: The Effect of varying Heat Source on Reservoir Temperature.

Figure 4.3.2 shows the effects of the varying heat source on viscosity. The decline in viscosity becomes rapid with a higher heat source. The lesser the heat source, the slower the decline because less energy is obtained by the molecules thus their movement is not faster.

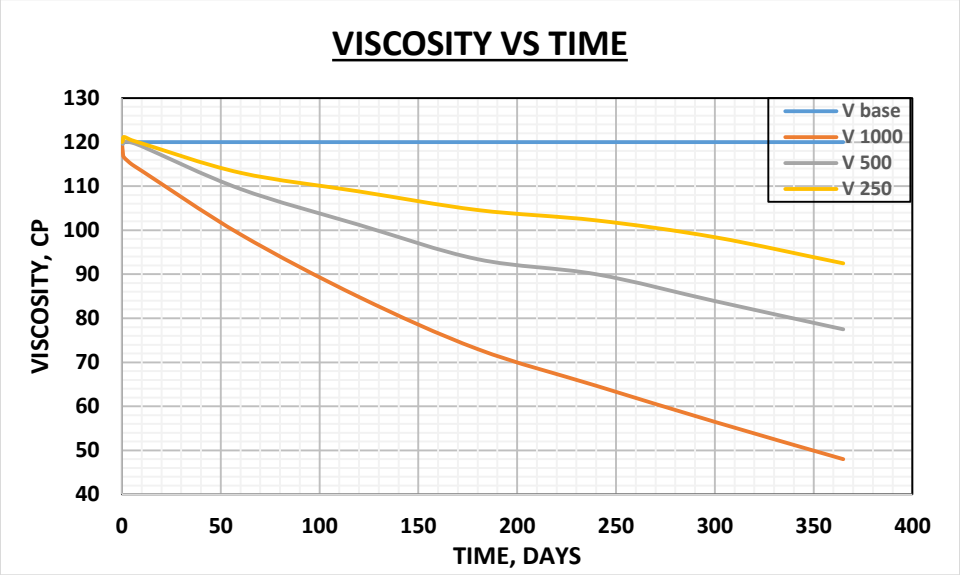

Figure 4.3.2: The Effect of varying Heat Source on Reservoir Viscosity.

Figure 4.3.3 depicts the behavior of the reservoir pressure with varying heat source. The higher heat source sustains the reservoir pressure which would prolong production life and recovery. As the heat source decreases, the pressure decline becomes fast since the viscosity drag effect is still high. The higher the heat source, the more rapid an increase in temperature occurs which results a rapid decline in viscosity and in turn decrease pressure slowly retaining enough to prolong the life of the reservoir.

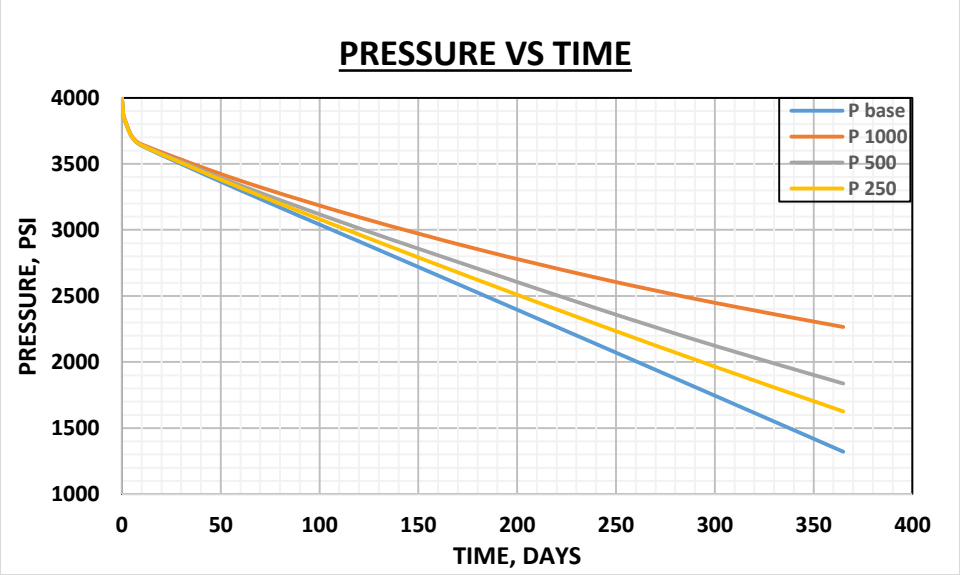

Figure 4.3.3: The Effect of varying Heat Source on Reservoir Pressure.

CHAPTER FIVE

CONCLUSION AND RECCOMMENDATION

5.1 Conclusion

In this work, a three dimensional numerical simulator for high viscous volumetric reservoir is developed. Key reservoir parameters such as temperature, viscosity, pressure and average pressure were evaluated using the developed simulator. The average reservoir pressure is determined as the weighted average. 2D plots of temperature, viscosity and pressure behavior with the introduction of a heat source over time were generated. Surface plots of the temperature increase, viscosity decrease and pressure depletion were generated considering some selected cells in the reservoir. Temperature plots showed a rise which was either rapid or gradual due to the amount of heat source introduced. Viscosity plots also showed a rapid or gradual decline depending on the effect from temperature which indicates an increase in mobility thus enhancing the hydrocarbons' sweep efficiency. Pressure behavior showed a slower pressure decline than the base case which has no heat addition thus pressure being sustained due to decrease in oil viscosity. The pressure behavior agrees with what literatures have proposed about enhanced oil recovery being used to maintain pressure and extend reservoir production life.

5.2 Recommendations

In order to make the developed simulator efficient, the following recommendations were made;

- Further studies should be done to analyze the effect of varying thermal properties with temperature such as thermal conductivity, specific heat capacity and density of the system since they are not constant.

- Change in temperature result in thermal expansion which affect the compressibility of the system which in turn affect the formation volume factor, permeability and porosity of the reservoir thus further studies can be made in evaluating the effect of varying compressibility, formation volume factor, permeability and porosity.
- Numerical methods such as finite element method, finite volume method, integral volume and variation method could be employed instead of the finite difference method used in this study for the discretization of the partial differential equation governing the whole system. This will accommodate both regular and irregular reservoir geometry.

REFERENCES

Abbas, F., *Thermodynamics of Hydrocarbon Reservoirs*, McGraw-Hill, 2000.

Ahmed T., Reservoir *Engineering Handbook*, Third Edition, Gulf Professional Publishing, 2006.

Archer, J.S., *Reservoir Definition and Characterization for Analysis and Simulation,* Preprint of the 11th World Petroleum Congress, London, England, 1983.

Arfo, Fatima, *EOR Lectures Notes,* African University of science and Technology, Abuja, 2014.

Aziz, K. and Settari, A., *Petroleum Reservoir Simulation*, Applied Science Publishers, 1979.

Cheng, Y., *Reservoir Simulation*, Department of Petroleum and Natural Gas Engineering, West Virginia University, USA, Encyclopedia of Life Support systems (EOLSS).

Ertekin, T., Abou-Kassem, J.H., and King, G.R., *Basic Applied Reservoir Simulation,* SPE Textbook Volume 10, 2001.

Ezekwe, Nnamdi, *Enhanced Oil Recovery Lecture Notes,* African University of Science and Technology, Abuja, 2011.

Fanchi, J.R., *Principles of Applied Reservoir Simulation*, Houston, Tex, Gulf Pub, 1997.

Finite Difference Methods, http://ltl.iams.sinica.edu.tw/document/training_lectures/2006/SH_Chen/Finite_Difference_Methods.pdf

Incropera, Frank P., De Witt, David P., *Fundamentals of Heat and Mass Transfer*, Third Edition, John Wiley & Sons, Inc., 1990.

Ismaila, N. Dele, Igbokoyi A.O., Kola, Babalola, *A Three-Dimensional Numerical Simulator for Expansion-Drive Reservoirs*, SPE (172368), Lagos Nigeria, August 2014.

Koederitz, L.F., *Lecture Notes on Applied Reservoir Simulation*, University of Missouri-Rolla, USA, 2004.

Latil, Marcel, Bardon, Charles, Burger, Jacques, Sourieau, Pierre, *Enhanced Oil Recovery*, Imprimerie Louis-Jean, Paris, 1980.

Mattax, C.C., and Dalton R.L., *Reservoir Simulation.* SPE Monograph Volume 13, Richardson, TX, 1990.

Ogbe, D., *Applied Reservoir Simulation Lecture Notes*, African University of Science and Technology, Abuja, 2014.

Omololu, Akin-Ojo, *Computational Modelling Lecture Notes*, African University of Science and Technology, Abuja, 2014.

Stone, H.L., *Iterative Solution of Implicit Approximations of Multidimensional Partial Differential Equations*, SIAM J. *Numerical Analysis*, 1968.

The MathWorks, Inc., *MATLAB: The Language of Technical Computing*, Getting Started with MATLAB Version 6, COPYRIGHT 1984 – 2001.

Thermal Conductivities, http://en.wikipedia.org/wiki/List_of_thermal_conductivities/2010.

NOMENCLATURE

A = Cross-sectional area normal in the direction of flow, (ft^2)

Δt = Time step (day)

Δx = Length of a grid block (ft)

Δy = Width of a grid block (ft)

Δz = Height of a grid block (ft)

H = Formation thickness (ft)

k = Rock permeability (d)

kx = Formation permeability in x-direction (d or md)

ky = Formation permeability in y-direction (d or md)

kz = Formation permeability in z-direction (d or md)

Lx = Formation length in x-direction (ft)

Ly = Formation length in y-direction (ft)

ϕ = Formation porosity (fraction)

C_t = Total compressibility

P = Reservoir pressure (psia)

$q_{i,j,k}$ = Oil flow rate from well in cell i,j,k (stb/day)

x = x-direction

y = y-direction

z = z-direction

Nx = Total number of grid cells in the x-direction

Ny = Total number of grid cells in the y-direction

Nz = total number of grid cells in the z-direction

δ = Partial differential operator

ρ = Density at reservoir condition

o = Oil

n = Previous time step

n+1 = Next time step

$\dot{m}$ = Mass flow rate,

ρ = Density,

Φ = Porosity,

u = Velocity,

q_s = Mass flow rate (sink term) of production

α_c = Volume conversion factor (to field unit) = 5.615

β_c =Unit conversion factor for permeability coefficient = 1.127

ρ_{sc} = Density at surface condition

ρ = Density at reservoir condition

V_{sc} = Volume at surface condition (stb)

V_b = Volume at reservoir condition (rb)

μ = Dynamic viscosity of the fluid (cp)

P = Pressure (psia)

Z = Elevation (ft)

γ = Fluid gravity (psi/ft)

B_o = Oil formation volume factor (rb/stb)

q = Volumetric flow rate of production (stb/D)

A = Transmissibility, (stb/day-psi)

S = Surface area

V = Volume of the system,

T = Temperature

k = Thermal conductivity of the system,

α = Thermal diffusivity of the system,

C_p = Specific heat at constant pressure,

ρ = Density of material used,

Q = Amount of heat in the system,

R = Heat flowing out of the system,

G = Heat generated within the system.

g = Heat Source